AN INVESTIGATION INTO THE LITHOLOGICAL SOURCE OF IRON IN THE KAMMANASSIE MOUNTAIN AQUIFER.

A thesis

Presented to

The Academic Faculty

By

Ruth Mitchell

In Partial Fulfilment

Of the Requirements for the Degree

Master of Science in Environmental Geochemistry

Department of Geological Sciences

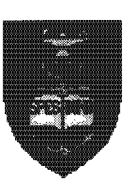

University of Cape Town

December 2003

ACKNOWLEDGEMENT

I would like to thank the following people for all their help throughout the year.

- Meris Smith my supervisor for hours of marking and all the moral support. Also to the other Environmental Geochemistry Lecturers, Dr Alakendra Roychoudhury and Dr John Compton, for all of their input.

- The staff of the UCT Geology Department particularly Andreas Spath, Patrick Sieas, David Wilson, Ivan Wilson, Ernest Stout and Robert Oliver for their help.

- Claire Laurence from the UCT Chemistry Department for running all of my samples on ICP-OES.

- All the people who have helped with the project from the Kammanassie Nature Reserve, in particular Peter Chadwick and Johannes Witbooi.

- The Environmental Geochemistry class of 2003 for all their support throughout the year, particularly Michael for pushing me over the edge and Róisín for bringing me back from it.

- To my family for always being there for me.

TABLE OF CONTENTS

LIST OF TABLES

LIST OF FIGURES

ABBREVIATIONS

bdl – below detection limit

DO – dissolved oxygen

DOC – dissolved organic compounds

DWAF – Department of Water Affairs and Forestry

EC – electrical conductivity

ICP-MS - Inductively Coupled Plasma Mass Spectrometry

ICP-OES – Inductively Coupled Plasma Optical Emission Spectrometry

KKRWSS – Klein Karoo Rural Water Supply Scheme

MAP – Mean Annual Precipitation

nd – no data

TDS – total dissolved salts

TMG – Table Mountain Group

XRD – X-ray Diffraction spectrometry

XRF – X-ray Fluorescence spectrometry

ABSTRACT

The precipitation of iron from aquifer water in boreholes is a problem in the Klein Karoo region of South Africa. The precipitation causes boreholes to clog and limits full use of well fields in the area. The iron is naturally occurring and this project sets out to identify the lithological source of the iron and in what form the iron is presented. The Table Mountain Group (TMG) aquifer is a fractured rock aquifer situated in the TMG and rock samples were taken from the various lithologies in the area. The rock samples were analysed for chemical and mineralogical composition as well as being used in leaching experiments. The leaching experiments were carried out using different leachates; organic water buffered at pH3, organic water buffered at pH5, water from borehole DL17 buffered at pH5 and de-ionised water. Water samples from boreholes in the region were analysed for iron concentrations and various other parameters.

The TMG is made up of the Peninsula sandstones, Cedarberg Shale and the Nardouw sandstone subgroup containing the Goudini, Skurweberg and Baviaanskloof Formations. It was found that the Goudini and Cedarberg Formations of the TMG contained the most iron (up to 6.5 and 6.8% respectively). Iron was however leached more easily from samples from the Goudini and Baviaanskloof Formations. Iron was more easily leached for these samples under anaerobic, low pH conditions in the presence of dissolved organic compounds (DOCs). Iron was found to be present as iron oxides (particularly haematite) between quartz grains as well as in fractures. Chlorite is also a possible suggested source of iron.

This study concludes that it is likely that the Goudini and Baviaanskloof Formations are sources of iron in the TMG aquifer however further research needs to be carried out especially on the Goudini Formations since its iron content is variable.

CHAPTER 1: INTRODUCTION

1.1 Introduction

The Table Mountain Group (TMG) aquifer is a valuable source of water for residents of the semi-arid Klein Karoo. Approximately 25 boreholes tap into this resource as part of the Klein Karoo Rural Water Supply Scheme (KKRWSS) and provide water to both municipal and agricultural users (Jolly & Kotze, 2002). However, the water yield has gradually decreased over time due to clogging of the boreholes by iron precipitation. Iron dissolved in the groundwater precipitates as it is brought up to the surface. Clogged boreholes are also commonly associated with biological fouling through development of a biofilm. The elevated concentrations of iron in the water and biofouling lead to problems in water extraction as well as poor water quality for users. Unfortunately remediation methods used in boreholes are harsh and expensive, so prevention would be better than cure (Jolly & Engelbrecht, 2002).

There is a lot of dispute about the source of iron in the TMG boreholes but very little is actually known about the geochemistry of the aquifer. Iron occurs naturally in the area but the specific lithological source is not known. It has been speculated that the iron originates from dissolution of minerals in the Nardouw Subgroup of the TMG or that the Bokkeveld Group is a source of iron in the area although there is no data to prove or disprove these claims (Smith *et al*, 2002, Kotze, 2000).

Many studies have been carried out on various aspects of borehole clogging in TMG aquifers although none on the source of iron in the water. If the source or sources of iron were identified this would aid in future borehole placement and well-field management. This study investigates the origin of iron in the groundwater from the

Kammanassie Mountain recharge area, with the aim of developing guidelines for future borehole placements as well as possible solutions to iron clogging in this area. The project is part of ongoing research to fully understand the borehole clogging problems in the area.

1.2 Objectives

The aim of this study is to determine potential sources of iron in the groundwater in the Kammanassie Mountain region. Specific objectives are to:

- Determine the mineralogical composition of various lithological units and identify which lithologies have the highest iron content.
- Determine lithologies from which the iron is most easily leached.
- Determine under which conditions iron is most easily leached and compare these to natural aquifer conditions.
- Compare iron concentrations in groundwater to the lithology from which the water is being extracted.

1.3 Background to Study

Set between the towns of Dysseldorp and Uniondale in the Klein Karoo (Figure 1.1 and 1.2) is the Kammanassie Nature Reserve, part of the larger Cape Nature Conservation body (Cape Nature Conservation, 2003).

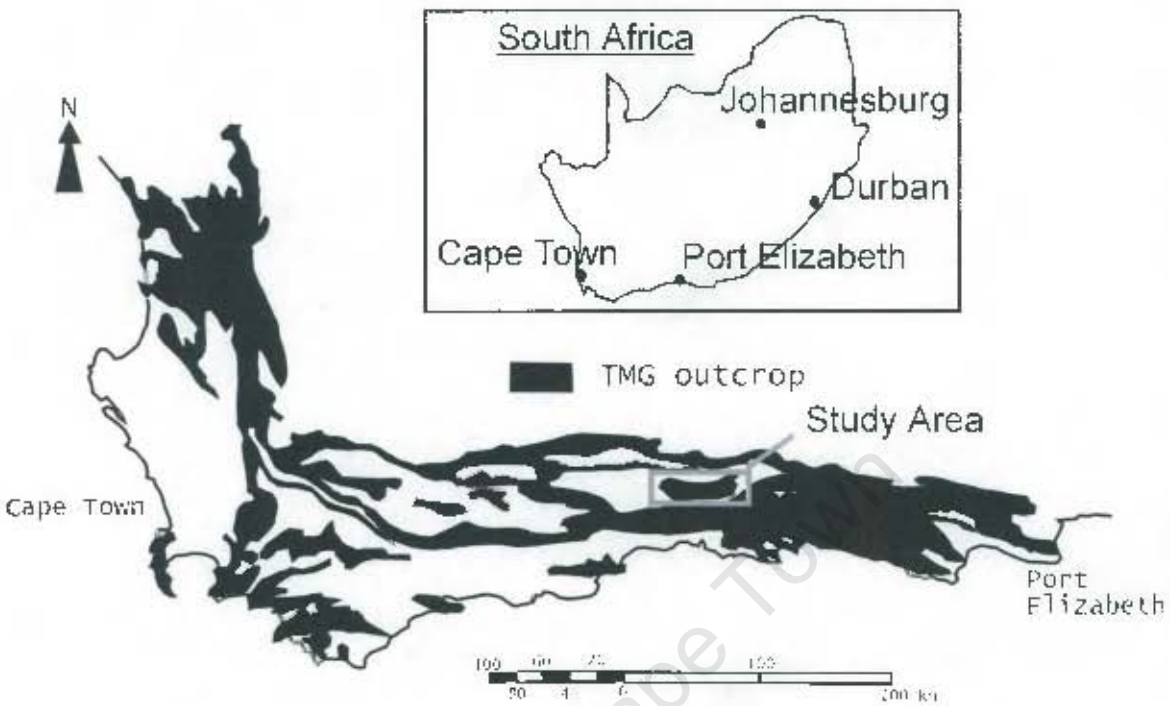

Figure 1.1: Location of the study area (see Figure 1.2) and the extent of the TMG (after Hartnady & Hay, 2002).

Figure 1.2: The larger study area (two sampling areas are indicated).

The Kammanassie Nature Reserve is a pristine mountain area that houses various flora and fauna including fynbos, kudu and the protected Cape mountain zebra. Vegetation generally consists of short scrubland and fynbos with small patches of afro-montane forest. The mountains reach an elevation of 1950 metres above mean sea level. The

climate in this area shows large diurnal and seasonal variations with summer highs up to 42ºC and winter temperatures dropping as low as -3ºC. The Klein Karoo tends to receive little precipitation but the high mountain areas such as the Kammanassie Mountains can receive up to ten times the amount of precipitation in the valley areas (Kotze, 2000). The mean annual rainfall of the Kammanassie Mountains is 550mm. These mountain areas provide a large portion of the recharge to the Table Mountain Group Aquifer. According to Kotze (2000), most of this precipitation occurs in the form of rain but in the higher mountain areas it can occur as snow.

The KKRWSS was established in 1984 to supply domestic water to the town of Dysseldorp and rural communities along The Olifants River (Kotze, 2000; Jolly & Kotze, 2002). The Department of Water Affairs and Forestry (DWAF) commissioned the supply scheme in order to supply water to areas with water shortages due to inadequate or irregular precipitation. It is the governments aim to supply adequate water for domestic needs to all people in the country and the KKRWSS is part of this initiative (National Water Act, 1998). About 25 boreholes have been drilled in the area and 18 have been used as full production boreholes. This well field is designed to supply up to 4.7×10^6 m^3/a, but current abstraction is considerably less at about 1.0×10^6 m^3/a. New projections indicate that the wellfield may only be capable of supplying 1.1×10^6 m^3/a (Kotze & Rosewarne, 1999). The current supply is equal to the demand in the area but poor wellfield performance may affect the future expansion of the water supply to meet the increasing needs of the people in the area. A reduction in borehole yields in recent years has been attributed to over-abstraction, biofouling and pump failure (Jolly & Kotze, 2002). It has also been suggested that over-abstraction is affecting the ecology of the Kammanassie Nature Reserve by depleting the flow of springs that are fed by the TMG aquifer (Yeld, 2002). Therefore widespread problems in the wellfield of the KKRWSS

seem to stem from an inadequate understanding of the aquifer from which the abstraction is taking place.

1.4 Hydrogeology

The sediments of the Cape Supergroup were deposited in shallow marine environments between about 500 and 340 million years ago (de Beer, 2002). These sediments are subdivided into the Table Mountain, Bokkeveld and Witteberg Groups and are exposed as the Cape Fold Belt which runs along the south and west coasts of South Africa (see Figure 1.1). The Cape Supergroup is made up of predominantly quartz arenites, shales and siltstones with minor conglomerate and a thin diamictite unit. Following deposition the sediments were indurated (hardened) and then fractured during the formation of the Cape Fold Belt. The fact that these rocks are well-fractured and relatively pure quartzites results in high quality groundwater ideal for development (de Beer, 2002).

1.4.1 Lithology

The TMG sandstones are subdivided into 3 main lithological units namely the Peninsula Formation, the Cedarberg Formation and the Nardouw Subgroup (Meyer, 1999). The Nardouw Subgroup is further divided into the lower Goudini, middle Skurweberg and upper Baviaanskloof Formations in the study area (see figure 1.3). Overlying the TMG in this area is the Bokkeveld Group, often with an abrupt contact (de Beer, 2002).

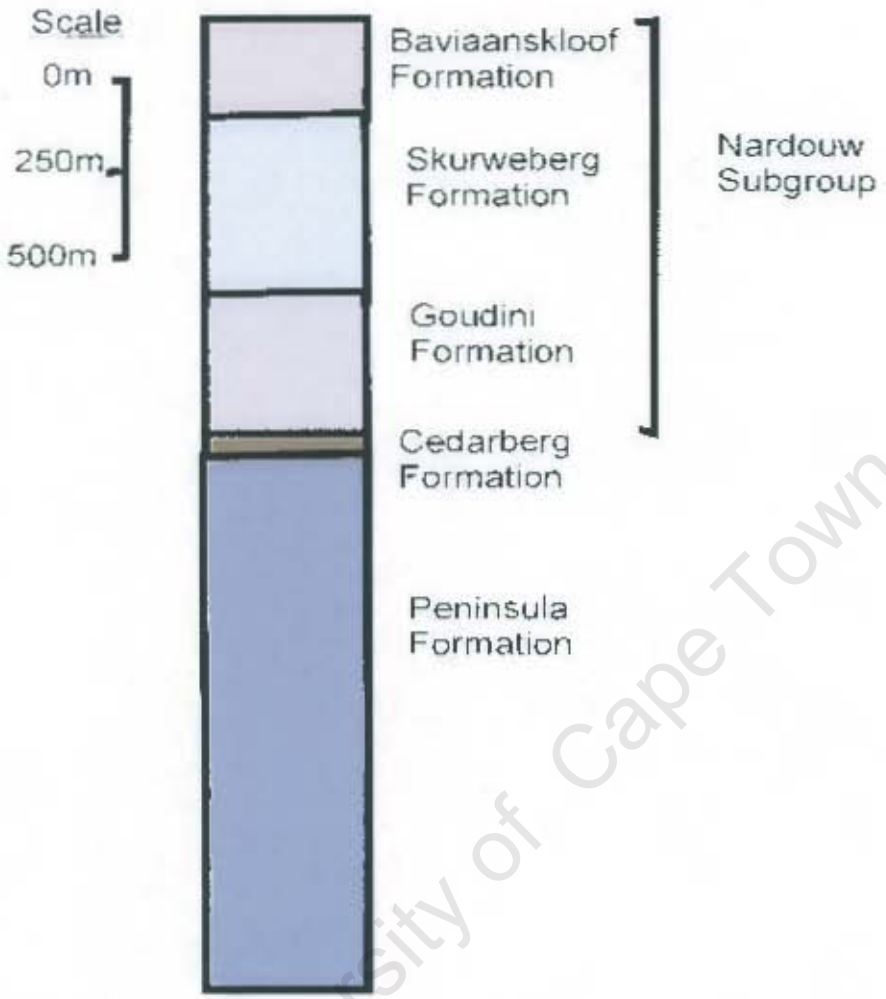

Figure 1.3: Stratigraphical column of lithologies in the study area.

The Peninsula Formation is the oldest formation of the TMG with an approximate thickness of 1500m (Meyer, 1999). It is made up of coarse-grained white quartz arenite with scatterings of small pebbles and thin layers of small pebble matrix supported conglomerate (de Beer, 2002). The pebbles are generally veined quartz. The Cedarberg Shale Formation is relatively thin at about 50m thick (Meyer, 1999). The formation consists of a black silty-shale at the base grading into a brownish siltstone with a fine sandstone at the top (de Beer, 2002). The Nardouw Subgroup is an approximately 900m thick sandstone layer varying between quartz arenite and silty and feldspathic arenites with small inclusions of conglomerate and shale (Meyer, 1999; de

Beer, 2002). The oldest Formation in this unit is the Goudini Formation with characteristic reddish coloured weathering and thin sandstone beds. Above the Goudini is the thick-bedded arenitic Skurweberg Formation that is more highly resistant to weathering and forms the highest peaks. The top unit is the Baviaanskloof Formation with a finer grain size than other units in the Nardouw Subgroup and high feldspar content. In Figure 1.4 it can be seen that the TMG sandstones are resistant to weathering and so make up mountainous areas, such as the Kammanassie Mountains (Kotze, 2000).

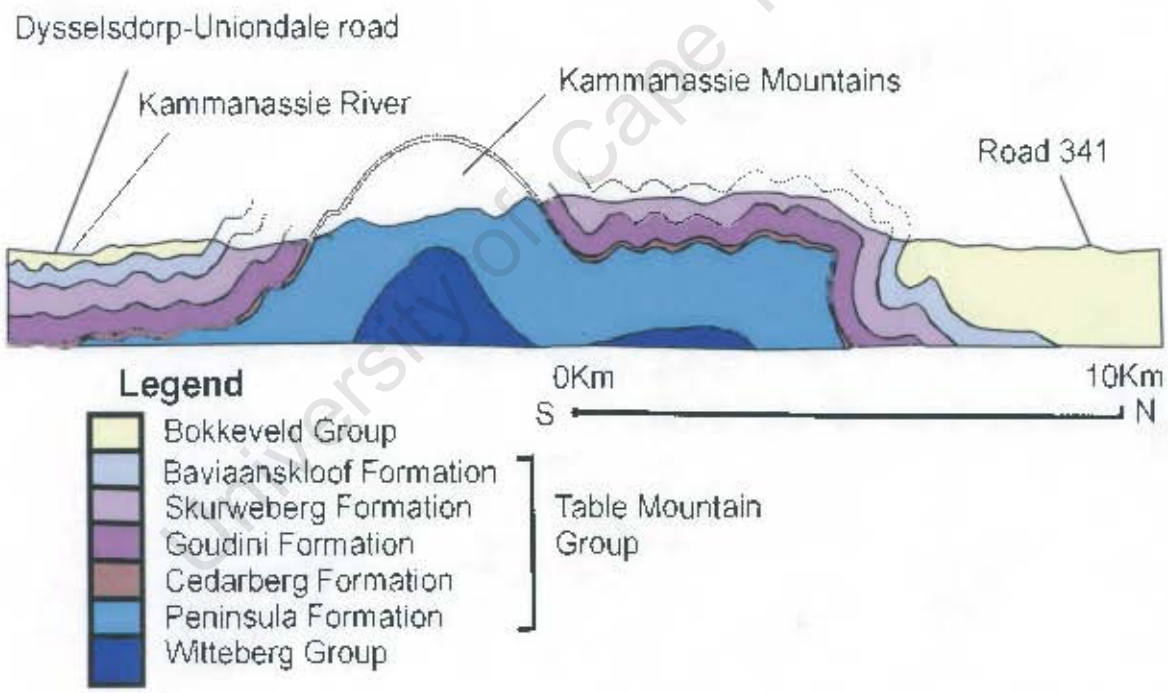

Figure 1.4: A geological cross section of the Kammanassie Mountains (after Kotze, 2000).

1.4.2 Fracturing

The TMG consists mainly of arenitic quartzite rocks that possess practically no primary hydraulic conductivity due to their highly indurated nature (Rosewarne, 2002). The TMG aquifer exists because of secondary hydraulic conductivity due to the fractured nature of the sedimentary rocks; the water lies within these fractures. Fracture systems were formed during the Cape Orogeny, but modern stress fields have an important influence on their ability to contain water by causing them to become more open or closed (Kotze, 2000). Therefore the orientation of these fractures in comparison to the direction of current regional extension is very important for their water holding capacity. Fractures that are perpendicular to the axis of regional extension, or at an acute angle to the direction of maximum compression are opened by the pressure and therefore have a greater capacity for water. There is a modern extensional regime trending WNW in the Klein Karoo; NNW fractures in the area are therefore more open and permeable to groundwater. Other fractures in the area trend ENE and NNE and so are unlikely to be opened up (Kotze, 2001).

1.4.3 Circulation Patterns

It is almost impossible to pin down specific figures for the storativity, transmissivity and hydraulic conductivity for the aquifer since it is so large and variable. It is thought that the aquifer possesses a deep regional groundwater circulation as well as smaller more localised circulations. Recharge occurs in the high-lying areas that receive higher rainfall and the water is circulated through the low-lying dryer areas. The TMG aquifer is therefore ideal for supply to the dryer valley areas (Kotze, 2000). The TMG aquifer is unconfined in the Kammanassie Mountains and is therefore susceptible to any pollution

that may occur at the surface. The inert quartzitic nature of the rock leads to water and soil of a poor buffering capacity, which also makes it more susceptible to pollution (Smart & Tredoux, 2002). Most of the recharge occurs in the higher-lying areas, many of which are nature reserves in pristine ecological condition and unlikely sources of pollution.

1.4.4 Hydrogeochemistry

Chemistry of groundwater is determined by the nature of lithological units and their structure. Groundwater chemistry will be affected by the lithology that contains the water and five groundwater zones with slightly differing chemical characteristics can be defined; Peninsula, 3 types of Nardouw (Goudini, Skurweberg and Baviaanskloof) and Bokkeveld. This study is concerned with the characteristics of the 3 types of Nardouw and the Peninsula groundwater zones. There is little connectivity between the 3 types of Nardouw and the Peninsula groundwater zones due to presence of the Cedarberg shale aquitard (Parsons, 2002). There may however be good connectivity in some areas where the consistent Cedarberg Shale has been fractured (Kotze, 2001). The aquitard also causes springs to develop which pass over it from the Peninsula Formation to the Nardouw Subgroup. Each of the aquifers has slightly differing water quality characteristics (Smith *et al.*, 2002).

1.4.5 Recharge

Recharge of an aquifer is a complex function of rainfall, snowmelt, topography and altitude, lithology, rivers, vegetation, fractures and groundwater variables. The recharge of this area is more dependant on single or multiple events rather than annual averages

since it is a semi-arid area. Quantification of recharge in fractured aquifer systems is difficult and there are varying literature values for the recharge of this area. Recharge of the TMG aquifer occurs mainly in the higher lying areas where up to ten times the precipitation of low-lying areas takes place (Kotze, 2000). In these high-lying areas recharge can be up to 20% Mean Annual Precipitation (MAP) as opposed to about 5% MAP in dryer areas (Parsons, 2002). Different lithological units may recharge at different rates with the more exposed unit, the Nardouw Formation set at 5% MAP and the sparse Peninsula Formation at 15% MAP (Kotze, 2000). The Peninsula Formation, therefore, plays an important role in the recharge to the local aquifers although there is little recharge of the Nardouw aquifer from the Peninsula since the Cedarberg Shale aquitard lies between them. Since the Cedarberg shale is an aquitard this means that although water can move through, it is at a very slow rate. Certain parts of the Cedarberg shale however are fractured and this allows for more easy movement of water through the shale layer (Kotze, 2000). It has been shown statistically and using stable isotopes that it is likely that the Nardouw and Peninsula aquifers have the same high altitude recharge source, with transfer from one to the other being the possible reason for this. The differences in water quality may be explained by enrichment of the Nardouw waters via evapotranspiration and water-rock interactions (Smith *et.al.*, 2002). Water from the Peninsula Formation has lower total dissolved salts (TDS) than the Nardouw Subgroup, which has been attributed to the higher feldspathic content and more profuse shale horizons in the Nardouw Subgroup (Kotze, 2000). A similarity between the water qualities of the two aquifers is probably due to connectivity through the Cedarberg Shale aquitard (Smart & Tredoux, 2002). These similarities and differences may affect the weathering capabilities of waters, which in turn affect the leaching of iron into groundwater.

Water from the TMG aquifer is considered to be generally of good quality due to its low electrical conductivity (EC) and therefore low TDS (Smart & Tredoux, 2002). The water is particularly characterised by a lack of calcium and magnesium (or low hardness). In general the water chemistry from the Peninsula and Nardouw aquifers is similar but there are some important differences (Table 1.1).

Table 1.1: Mean chemical analyses from the Nardouw and Peninsula aquifers (after Smith *et al.*, 2002)

	Peninsula	**Nardouw**
EC (mS/m)	10.4	30.0
pH	6.2	6.0
Na (mg/l)	11.1	30.8
Cl (mg/l)	18.0	56.2
Alkalinity as $CaCO_3$ (mg/l)	14.5	42.8
Fe (mg/l)	0.2	3.3

TMG groundwater is classified as Na-Cl dominant. The waters are poorly buffered because of the low alkalinity and this is apparent from the wide pH range measured in all formations. A low buffering capacity makes them highly susceptible to pollution. The waters have also been shown to be generally acidic and soft which makes them corrosive to pump fittings and aggressive to cement (Mackintosh & de Villiers, 2002). In terms of this study, the most important aspect of groundwater quality is the dissolved iron content. Iron concentrations have been found to be generally low with an increase towards the Cedarberg Shale Formation contact (Smart & Tredoux, 2002). Iron

concentrations are highly pH dependant and generally show an increase with a decrease in pH (McBride, 1994). The Nardouw waters have been shown to have up to 21 times more iron than Peninsula waters (although this is variable) and it has been suggested that pyrite and illite in the Nardouw Subgroup or the Cedarberg Shale Formation may be the reason for this. There may be inaccuracies in some of these measurements however due to the fact that it is impossible to get a pure aquifer sample since the water is affected by being pumped out of a borehole. If a sample is unfiltered, precipitated iron flushed out of a borehole during pumping will greatly exaggerate the results (Smith, 2003, pers com.)

1.5 Iron Geochemistry

1.5.1 Iron Cycling in Aquifers

Dissolved iron occurs naturally as two redox species; as the ferric iron (Fe(III)) in oxidising environments or as ferrous iron (Fe(II)) in reducing environments. The oxidation or reduction of iron is controlled by redox potential (pe) and pH which in turn are affected by the presence of organic matter, dissolved oxygen and microorganisms (Smith & Tuovinen, 1985). Fe(III) is sparingly soluble except at low pH and primarily occurs as a precipitate whereas Fe(II) is generally soluble in reducing environments (Figure 1.5). Borehole waters in the TMG have been found to lie along the line separating $Fe(OH)_3$ and Fe^{2+}, the Fe(III) is solid and the Fe(II) is dissolved. The Eh and pH of stagnant waters in boreholes is controlled by iron oxidation and precipitation of ferrihydrite. This data suggests a pe in the fresh water of approximately 3 (Cavé & Smith in prep). Redox levels in groundwater are controlled by the amount of dissolved oxygen that is present and the consumption of oxygen by the bacterially mediated

decomposition of organic matter (Drever, 1997). Ferric oxyhydroxide reduction is an important groundwater process:

$$C_{organic} + 4Fe(OH)_3 + 8H^+ = CO_2 + 4Fe^{2+} + 10H_2O$$

(Drever, 1997)

The Fe^{2+} produced may stay in solution or it may precipitate out. Fe^{2+} will be oxidised with an increase in pH and/or Eh:

$$Fe^{2+} + 3H_2O = Fe(OH)_3 + 4H^+$$

(Drever, 1997)

High levels of dissolved organic matter in the TMG waters (up to 16mg/l) may inhibit the re-precipitation of iron in the groundwaters but may aid in the precipitation of ferrihydrite ($5Fe_2O_3.9H_2O$) under rapidly oxidising conditions. Since the iron oxide precipitates in TMG boreholes were found to be mainly ferrihydrite (Miller, 2001) this may explain the basic pathway of iron in the aquifer. The rapidly oxidising conditions can be caused by bringing water up to the surface in boreholes or oxygenation via physical cascading when boreholes are pumped to below water strike levels (Smith, 2002).

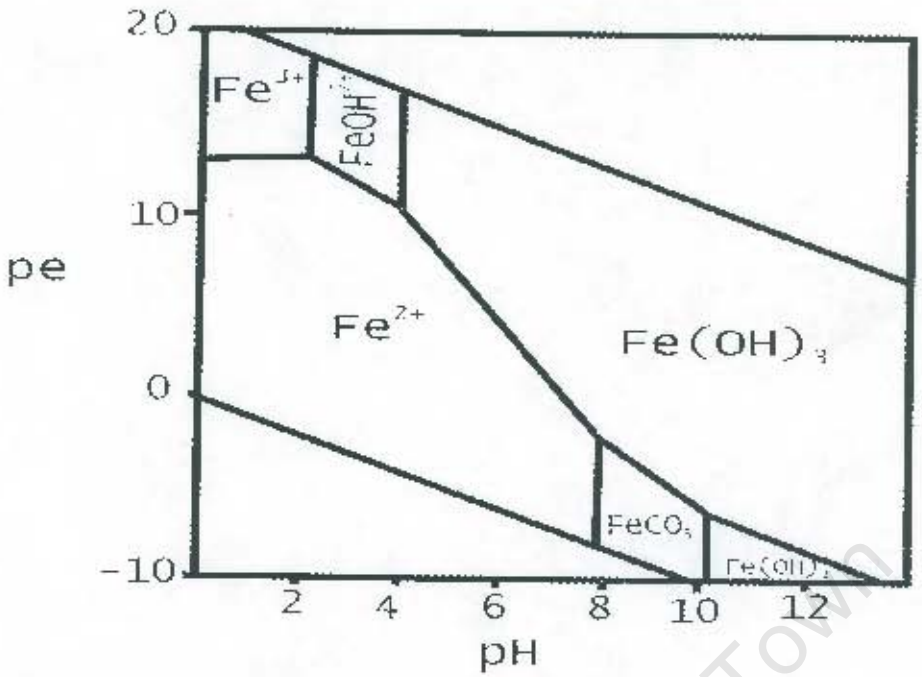

Figure 1.5: pe-pH diagram for iron (McBride, 1994)

Over the pH range of natural waters (5-9) as conditions become reducing, dissolved iron concentrations increase (Drever, 1997). This trend is reversed if there are sulphate species present and the redox level where sulphate reduction occurs is reached. This is because iron sulphides will then be formed and precipitate out. If sulphates are absent iron concentrations are controlled by the solubility of $FeCO_3$ (Drever, 1997).

Water enters the soil and dissolves organic compounds (DOC), some of which will be organic acids, from the soil and from plants (see Figure 1.6). As the water percolates down through the soil and into the aquifer conditions become gradually more anoxic due to depletion of O_2 by oxidation of DOC. Apart from contributing to the development of reducing conditions, DOC molecules also higher the solubility of iron by complexation. Fe^{3+} is reduced to Fe^{2+} under anoxic conditions and the DOC can aid in this transformation by donating an electron and itself becoming oxidised. Iron can also

dissolve without the help of DOC. Once the dissolved iron is in the aquifer water it is mobilised and will only precipitate out under oxidising conditions such as occur in a borehole, or more reducing conditions as iron sulphides. In a borehole under oxidising conditions Fe^{2+} is oxidised to Fe^{3+}, which often precipitates as an iron oxide causing clogging. Iron bacteria act as biological catalysts and speed up the oxidation reaction.

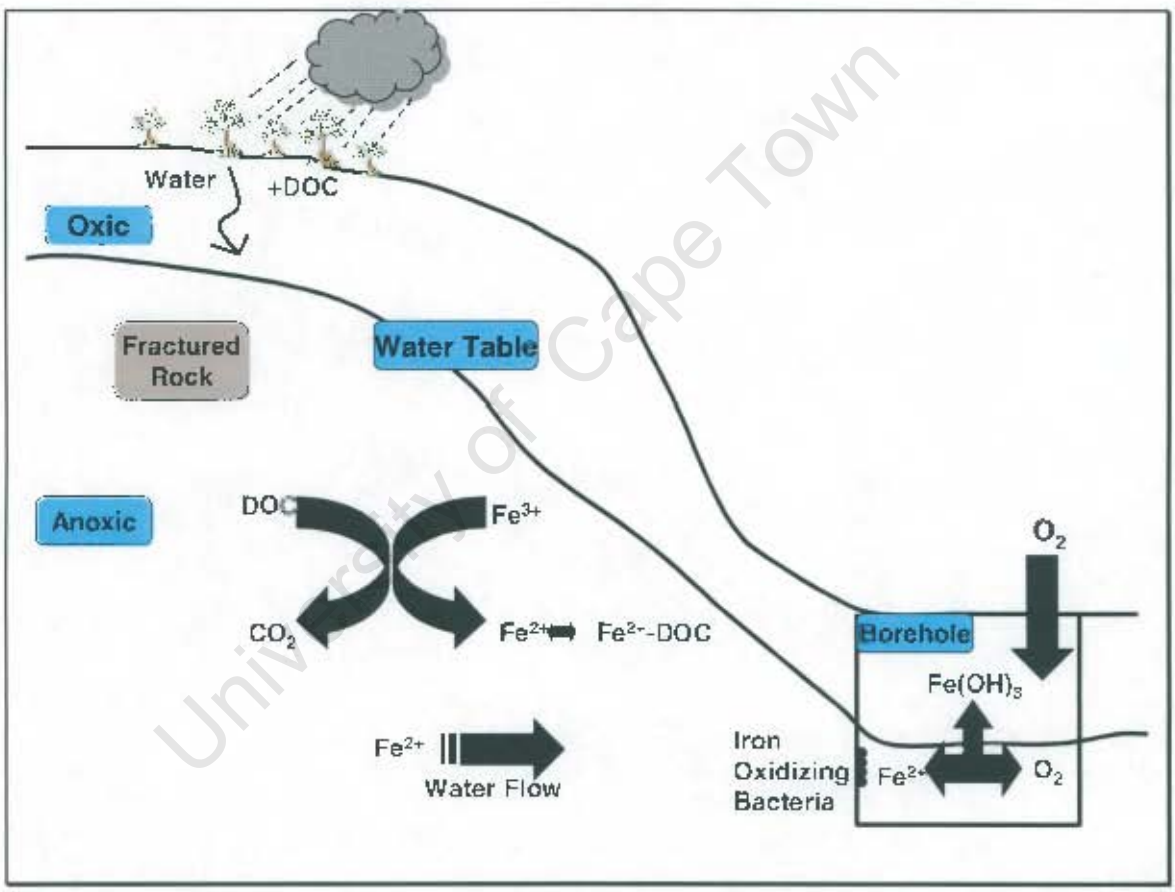

Figure 1.6: A schematic diagram of iron cycling in aquifers.

1.5.2 Iron Clogging

The problem of iron related biofouling is an international one but literature on it tends to be sparse (Smith, 2002). In South Africa biofouling is particularly associated with the

boreholes in the TMG aquifer and in Atlantis (Smith *et.al.*, 2002). Biofouling has led to the clogging of pumps and borehole screens and therefore a decrease in borehole efficiency and yield (Jolly, 2000). The deposits consist mainly of iron hydroxides, organic matter and water (Tyrrel & Howsam, 1990) and appear as a crust on the inside of pipes and on screens (see Figure 1.7). In other parts of the world these deposits have also been associated with manganese, but this is not the case here possibly due to the lower concentrations of naturally occurring manganese. In the case of iron biofouling the iron that is dissolved in the groundwater under anoxic conditions is oxidised (to Fe^{3+}) as it is brought to the surface. Iron precipitates in the form of iron oxyhydroxides and is often associated with biological clogging (biofouling) (Jolly & Engelbrecht, 2002). This association is because microbes catalyse the naturally occurring oxidation of Fe^{2+} (Miller, 2001). When iron precipitation is associated with biofouling it has been found to occur rapidly and cause severe clogging (Jolly & Engelbrecht, 2002).

Figure 1.7: A clogged pipe, showing layers of precipitate within the pipe (Miller, 2000)

1.5.3 Sedimentary Source Minerals of Iron

Minerals in sedimentary rocks can be derived from the original grains laid down in the sediment or may precipitate from the porewaters during diagenesis. The origin of the minerals becomes complicated when one sedimentary unit becomes overpressured and retains high volumes of porewater. The porewaters may evolve due to water-rock interactions during progressive burial. At some later stage during burial, overpressure may become released and the evolved porewater may flow upward through overlying strata. The porewater may then be involved in progressive water-rock interactions in the overlying strata (de Caritat & Baker, 1992). This means that adjacent sedimentary units should share some common attributes, especially parts of those strata that are in contact with the lower strata.

Iron can be found in many minerals such as pyrite (FeS_2), goethite (FeOOH) and magnetite (Fe_3O_4). Dissolution processes from these minerals will all be different and dependent on various factors. For most iron containing minerals the iron is reduced and released, however pyrite is different. In pyrite the sulphide will be oxidised to SO_4 and the iron (which is already in the reduced state) will be released into the water in the Fe^{2+} form. It has been suggested that pyrite found in fractures in the TMG is a possible source of iron although the groundwater was found to be highly undersaturated with respect to pyrite (Smith *et al.*, 2002). Other possibilities are iron-substituted clay minerals such as mica or illite. The Nardouw (especially the Baviaanskloof Formation) and Cedarberg are the most clay rich in the TMG and therefore possible sources of iron-substituted clay minerals (de Beer, 2002).

Iron oxides such as goethite (FeOOH) and haematite (Fe_2O_3) are common sources of iron in sediments. Most haematite is secondary, occurring as a weathering product of iron containing minerals. Haematite can also form as a diagenetic product of iron-rich sediments. Haematite is an iron oxide, with minor MnO and FeO included in the structure (Deer *et al*, 1992). Haematite may also contain titanium in the form of titanohaematite. Goethite also occurs generally as a weathering product, in particular from iron containing minerals such as siderite, magnetite and pyrite (Deer *et al*, 1992).

Although pH is important it is not the only variable affecting the weathering of iron from rock. The organic content of the water leachate may affect the rate of leaching (Heyes & Moore, 1992). Organic particles bind tightly to Fe^{3+} and Fe^{2+} and so aid in the weathering of iron containing rocks. The leaching of both Fe and Al have been linked to high DOC (dissolved organic carbon) in water. In the same set of research it was however found that although the DOC content speeds up the leaching of iron, anaerobic conditions did not affect the results a great deal (Heyes & Moore, 1992). This is in contradiction to other literature, which suggests that dissolved iron content increases as conditions become anaerobic (Drever, 1997). In soils it is suggested that the weathering of chlorite in particular is accelerated by organics. These organics form complexes with iron and remove it from the chlorite as the organic solution percolates downward (Bain, 1976).

With information on the chemical and mineralogical compositions of the different formations in the TMG as well as the leaching of iron from the rocks, the lithological source of iron should be identified. Knowledge of the source of iron will aid in future borehole placement and current well field management.

CHAPTER 2: FIELD SAMPLING AND LABORATORY METHODS

2.1 Borehole Water Samples

Water samples were collected from the 8 boreholes near the Kammanassie Mountains as well as near Calitzdorp (Figure 2.1).

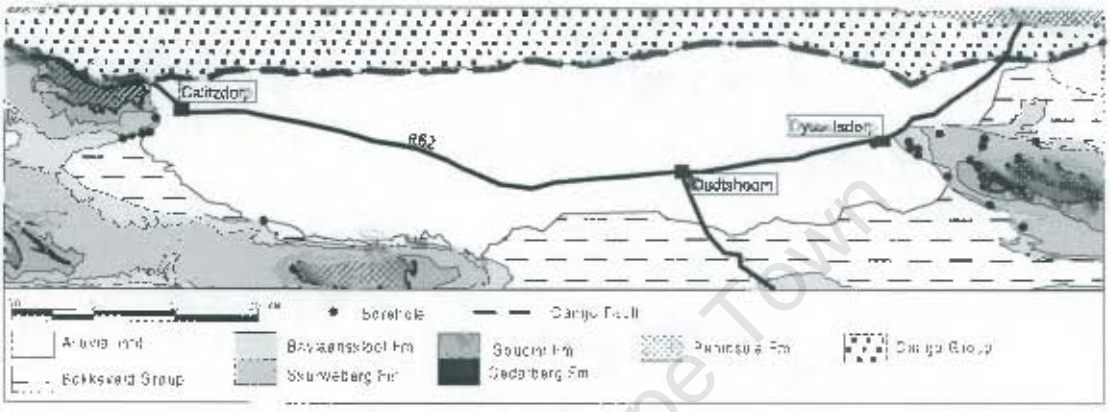

Figure 2.1: The Calitzdorp and Dysselsdorp well fields.

The boreholes were in production when sampled and therefore did not need to be purged. The Stratigraphy of the borehole was roughly determined using geological maps in order to estimate the origin of the water. Basic parameters of the water were measured in the field: pH, temperature and dissolved oxygen (DO). Water samples were collected, filtered and acidified in the field. The ferrozine method was used in the field to determine concentrations of Fe(II) and total iron in the waters. This method involves the use of ferrozine in a buffer and a reductant. HEPES buffer (12g) and ferrozine (0.2g) in one litre of water makes up the ferrozine reagent, which is adjusted to pH7. This produces a purple colour in the presence of Fe^{2+} that can be measured in a spectrophotometer at 562nm. To measure total iron a reductant (made up of 1g hydroxylamine HCl in 100mL of the ferrozine reagent) is used. The concentration of

Fe3+ was determined by difference (modified from Viollier *et al*, 2000). Total iron was also determined using ICP-MS from samples which were refrigerated in plastic bottles for less than a month. The same samples were also sent for dissolved organic carbon (DOC) analysis at CSIR Environmentek in Stellenbosch, South Africa.

2.2 Lithological Samples

Lithological samples were collected from twenty-four different sites along the Kammanassie Mountains representing 6 different formations namely: Peninsula, Cedarberg, Skurweberg, Goudini, Baviaanskloof and Bokkeveld Formations (Table 2.1). The samples were taken on a transect along the eastern side of the mountains (Figure 2.2) and a transect along the western side of the mountains (Figure 2.3). Two additional samples were taken from the Calitzdorp area. Sample sites were recorded as well as the visual setting of the sample. An attempt was made to collect fresh samples but some Formations such as the Baviaanskloof were deeply weathered. Due to the fact that the sampling was carried out in a pristine nature reserve care was taken to disturb the natural surroundings as little as possible.

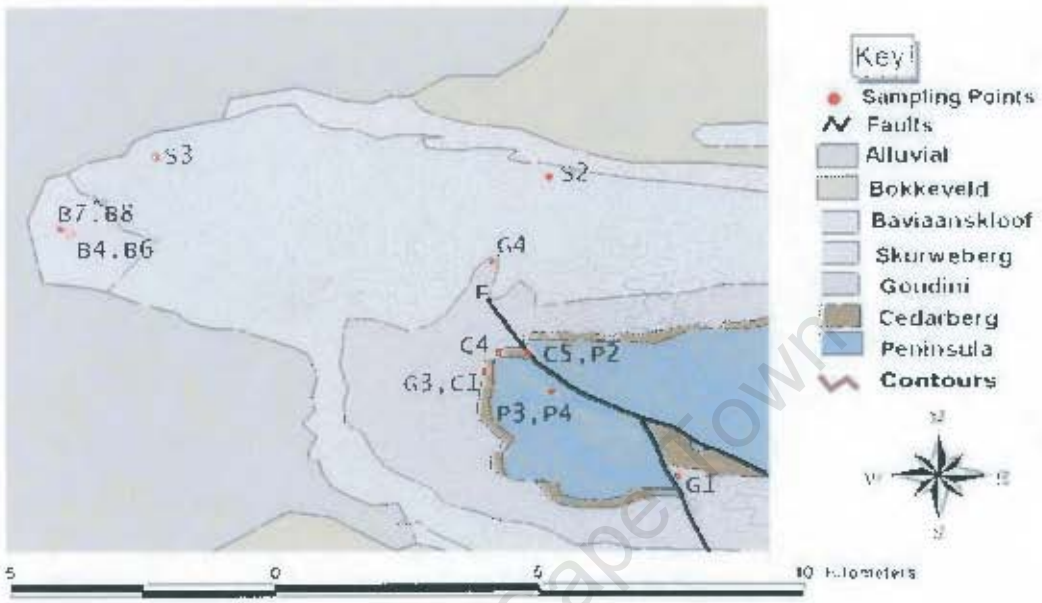

Figure 2.2: Sample sites in Sampling area A (see Figure 1.2).

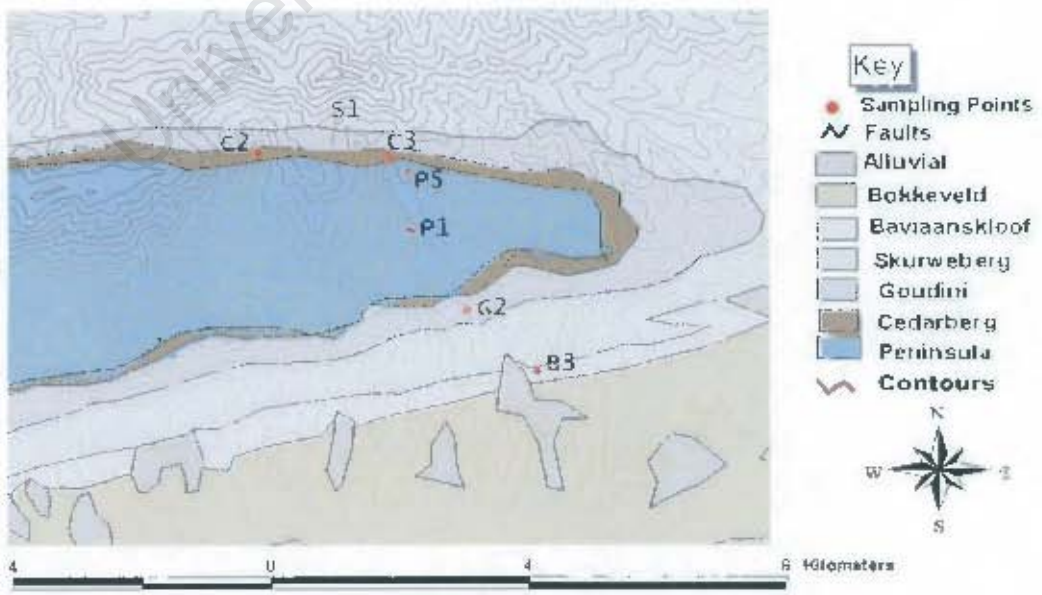

Figure 2.3: Sample Sites in Sampling Area B (see Figure 1.2).

Table 2.1: Site description of samples and their coordinates.

Sample	Latitude and longitude	Site Description
P1	33.6366° S, 22.95036° E	Peninsula Formation from the eastern side of the Kammanassie Mountains.
P2	33.6033° S, 22.53185° E	Peninsula Formation from a fractured outcrop near the Peninsula-Cedarberg contact on the Western side of the Mountains.
P3, P4	33.6091° S, 22.53798° E	Peninsula Formation sampled adjacent to each other on the western side of the mountains. Weathered colour was rusty to yellow colour, with fresh sample being a whitish-grey.
P5, P6	33.6295° S, 22.94794° E 33.6431° S, 22.95279° E	Peninsula Formation sampled on the Eastern side of the Kammanassie Mountains.
C1, C4, C5	33.6033° S, 22.52969° E 33.6032° S, 22.53028° E 33.6033° S, 22.53185° E	Cedarberg shale taken along a cross section on the western side of the mountains. C1 was taken from next to the Cedarberg-Goudini contact, C4 was taken from an outcrop of more resistant shale in the middle and C5 was sampled next to the Cedarberg-Peninsula contact.
C2, C3	33.6232° S, 22.92838° E 33.6289° S, 22.94782° E	These were sampled on the eastern side of the mountains. There was a visible depression where the weaker shale had been weathered and eroded between the more resistant sandstones. Sample C3 was taken on an outcrop and was highly weathered. C2 was sampled along a road cutting

		and was fresh. In the road cutting clear bedding structures could be seen. The weathered Cedarberg Shale had a characteristic orange-yellow colour and was soft whereas the fresher sample was darker and grey-green.
G1	33.617° S, 22.55375° E	Goudini sampled in a riverbed along a fault on the western side. The rock showed iron banding (Figure 2.4) within white-grey sandstone.
G2	33.6491° S, 22.95662° E	Goudini sampled along the eastern side of the mountains.
G3	33.6033° S, 22.52969° E	Goudini along a transect and was taken next to C1 (at the Cedarberg- Goudini contact).
G4	33.5789° S, 22.53306° E	Goudini Formation sampled next to the Vermaaks River on the western side. The rock shows dark red/brown weathering and is highly resistant to weathering.
S1	33.6254° S, 22.93891° E	Skurweberg from the eastern side of the Kammanassie Mountains. It is a clean white sandstone that forms cliffs that are resistant to weathering.
S2	33.5673° S, 22.53836° E	Skurweberg sampled on the western side of the Kammanassie Mountains near borehole VG3. Orange-brown weathered with fractures. Fresh samples are grey to white.
S3	33.5666° S, 22.47051° E	This Skurweberg sample was sampled near

		borehole DG110.
B4, B6	33.5806° S, 22.45579° E	These Baviaanskloof samples were taken on the
	33.5801° S, 22.45497° E	western side.
B7, B8	33.5801° S, 22.45497° E	Baviaanskloof Formation sampled near borehole DP15 on the western side. The samples are weathered and dark in colour.
B1, B2	33.5595° S, 21.6393° E	Bokkeveld Shale sampled near borehole DL16 near Calitzdorp.

Figure 2.4: Iron banding in the Goudini Formation where sample G1 was taken.

2.2.1 Mineralogical and Chemical Composition

Weathered edges were removed and samples were split using a rock splitter. The freshest parts of the sample were then crushed using a jaw crusher. Finally the samples were ground for 1 or 2 minutes (depending on their competence) using a carbon-steel Seib mill. Major elemental composition was determined by XRF using fusion discs. Approximately 2g of each powdered sample was weighed out into a crucible. The samples were dried for four hours at 110ºC, weighed, roasted overnight at 850ºC and re-weighed to determine water and LOI (loss on ignition). Of each sample 0.7g was weighed and added to 6g of flux (lithium tetraborate; dried overnight at 450ºC) to make fusion discs with a Claisse Fluxy. The fusion discs were analysed using an X'Unique Philips XRF Spectrometer.

The mineralogy of the powdered samples was determined using a Phillips X-Ray diffractometer with a copper k-α tube with a wavelength of 1.542Å at 40kV and 20mA. The samples were all analysed from $2\theta = 5^{\circ}$ to $2\theta = 70^{\circ}$.

Thin sections were prepared from each individual lithological sample and these were analysed under a microscope in order to determine the mineralogy.

2.3 Leaching Experiments

2.3.1 Trial Leaching Experiments

Two trial leaching tests were run in order to determine parameters for the running of actual leaching tests. Lithological samples G1 and C2 were used since G1 was presumed to have high iron levels and C2 low iron levels. In the initial test organic rich water (from the Palmeit river) was used as the leachate since literature suggests organics increase the amount of iron leached (Heyes & Moore, 1992). The organic content of the water is 16mg/l. 0.5g of each sample was weighed out into a test-tube and 10ml organic water was added. For each lithological sample ten discrete test tubes were used to be sampled at different times. For the first leach trial the times were 10 and 40 minutes, 1:40, 3:40, 7:40 and 23:40 hours. After each time period one test-tube from each lithology was removed and placed in a centrifuge for 5 minutes in order to separate the sediment from the leachate. Samples were then filtered through 0.45µm filters and measurements of pH and temperature were taken before the sample was acidified using nitric acid. Iron concentrations in the leachate were measured using ICP-OES The machine used is a Jobin Yvon JY70C (combination simultaneous-sequential) inductively coupled optical emission spectrometer (ICP-OES).

The second trial leach test was carried out to determine the difference in leaching properties between the organic water used in the first trial and de-ionised water. Samples of the same lithologies were prepared using the same method as above, adding 10ml of de-ionised water instead of organic water. The same samples were run over a shorter time period: 10 and 40 minutes, 1:40, 3:40 and 7:40 hours. Separate test tubes were also prepared containing different ratios of organic and de-ionised water for

each lithology. The ratios of organic to deionised water were 1:3, 1:1 and 3:1. These were then compared with pure organic and pure de-ionised leachates. The samples were treated and analysed as in the first trial.

2.3.2 Aerobic and Anaerobic Leaching Experiments

Literature suggests that the amount of oxygen in a leachate may affect the amount of iron being leached out (Heyes and Moore, 1992). Since an aquifer is under anaerobic conditions the amount of oxygen in the water and it's effects is important to consider. The following leach experiments were designed in an effort to test the effects of oxygen content in water on the leaching of iron from TMG rocks.

The aerobic leach experiment was designed from the results of the two trial leach tests. In the trial leach tests it was found that the pH varied greatly and that colloidal iron passed through 0.45µm filters. Because of this it was decided to buffer the waters and to use 0.2µm filters for further leaching experiments. Leaching experiments were carried out on 4 lithological samples- Cedarberg (C2), Goudini (G1), Bokkeveld (B1) and Baviaanskloof (B7). The samples were leached over a period of 5 days with samples being taken at 10 and 40 minutes, 1:40, 3:40, 7:40, 23:40, 47:40 and 95:40 hours. Each sample was leached individually with de-ionised water, organic water buffered at pH 3, organic water buffered at pH 5 and borehole water from DL17 (in the Calitzdorp area) filtered and buffered at pH 5. In addition samples C1, P5, B2 and B4 were leached for the full five days using all leachates to determine the consistency of results through the same lithology. Duplicates were added to determine the reproducibility of the results. The samples were filtered using 0.2µm filters and analysed using ICP-OES.

Samples G1, P5, C1, C2, B1, B2, B7 and B4 were leached for a total of 4 days under anaerobic conditions, using an anaerobic chamber filled with nitrogen. Each sample was leached using de-ionised water, organic water buffered at pH3, organic water buffered at pH5 and borehole water from DL17 (in the Calitzdorp area) filtered and buffered at pH5. Due to limitations samples were analysed only after the full time (95 hours) samples were filtered using 0.2µm filters and analysed using ICP-OES. Ideally the samples would have been analysed at time intervals.

2.3.3 Total Reactive Iron

A determination of the total reactive iron was carried out on all the lithological samples. The leach is able to extract all iron oxides except magnetite. Magnetite and iron associated with silicates can be released if leached over a longer period of time (Roychoudhury *et al*, 2003). The leachate used consisted of a buffer solution made up of 0.2M sodium citrate and 0.35M acetic acid. To every 10ml of buffer solution 0.5g sodium dithionite was added. In order to determine the success of the total leach samples were taken after 2 and 3 days. They were then analysed using ICP-OES.

CHAPTER 3: RESULTS

3.1 Water Samples

Water samples were taken from boreholes in the Calitzdorp and Dysselsdorp well-fields. There was found to be high levels of iron in boreholes KG1, DP15 and DL17. Spring water was found to contain little iron (Figure 3.1). The ferrozine method showed that most borehole samples did not only contain dissolved (Fe^{2+}) iron (Figure 3.2). Boreholes KG1 and DL17 also contained high levels of manganese and again spring water contained little manganese (figure 3.3).

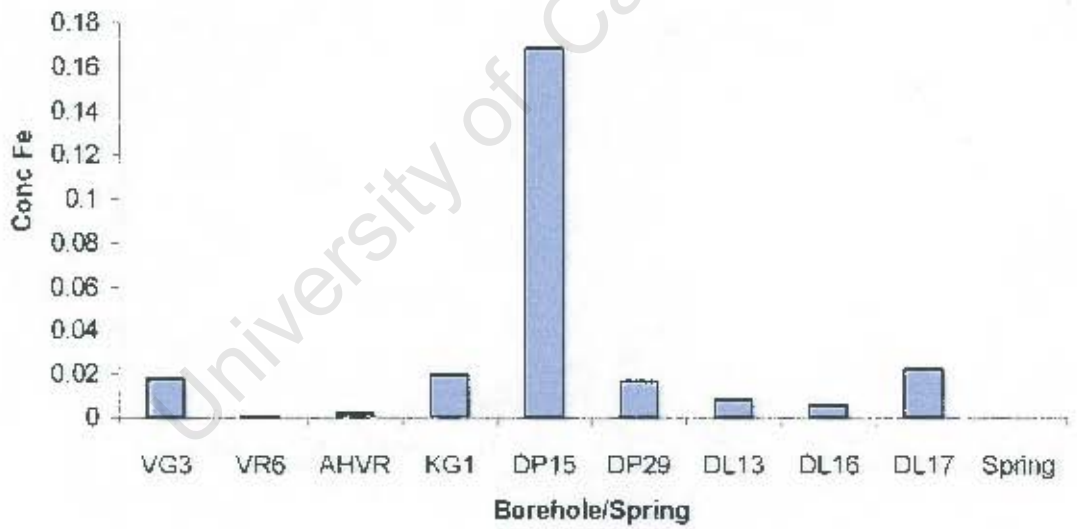

Figure 3.1: Concentration of iron in spring and borehole water samples (from ICP-MS, see Appendix for data).

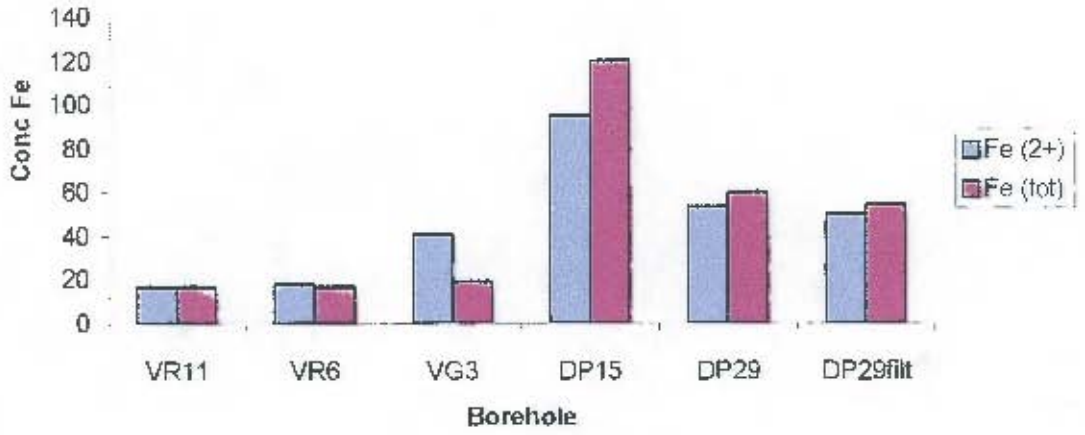

Figure 3.2: Iron speciation in boreholes using the modified ferrozine method.

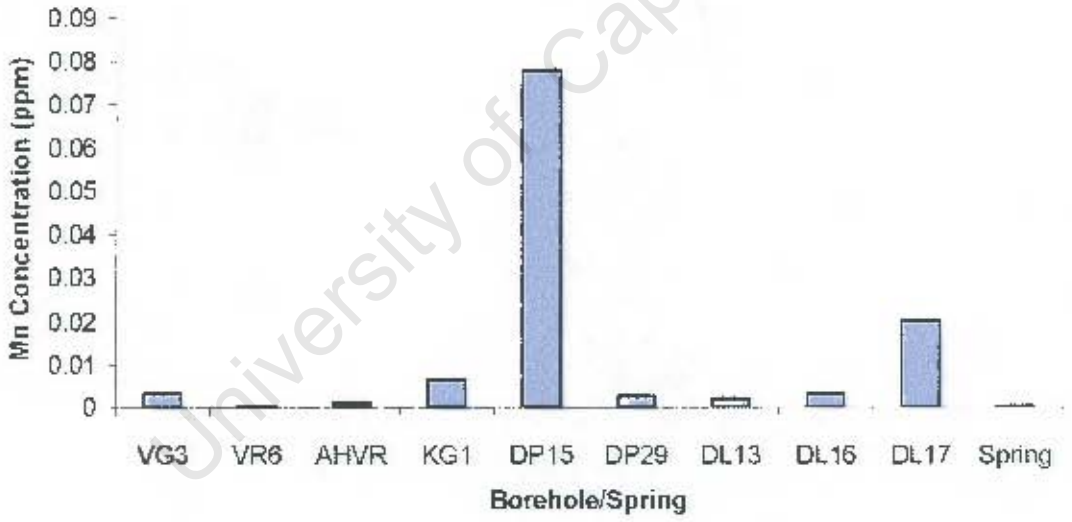

Figure 3.3: Concentration of Manganese in spring and borehole water samples (from ICP-MS, see Appendix for data).

There was found to be little DOC in all borehole samples except for borehole DL16 (Table 3.1). The spring water had low levels of DOC. Organic water had high levels of

DOC but these decreased after being passed through a 0.45µm filter. No relationship was observed between pH and iron concentration in the data.

Table 3.1: Dissolved organic carbon concentrations in water samples. Organic water samples are from the Palmiet River.

Water Sample	Dissolved Organic Carbon (mg/l)
KG1	<1
Spring	2.1
DP29	<1
DL13	3.0
Artesian Borehole (AHVR)	<1
VG3	<1
DP15	<1
DL16	6.4
DL17	<1
VR6	<1
Organic Water (unfiltered)	16
Organic Water (filtered)	11

There are few drilling logs available for the boreholes that were samples and those that are available are at low resolution. The Stratigraphy of the boreholes was therefore estimated from the 1:10 000 geological map. Most of the boreholes with historic iron

clogging problems appear to be sourced in the Baviaanskloof and Goudini Formations (Table 3.2).

Table 3.2: Stratigraphy of boreholes

Water Sample	**Historical Incidence of Clogging?**	**Estimated Geological origin of borehole.**
KG1	Yes	Baviaanskloof Fm.
Spring	N/A	Skurweberg Fm.
DP29	Yes	Baviaanskloof Fm.
DL13	Yes	Peninsula Fm.
Artesian Borehole (AHVR)	No	Peninsula Fm.
VG3	No	Peninsula Fm
DP15	Yes	Skurweberg Fm.
DL16	Yes	Goudini Fm.
DL17	Yes	Goudini Fm.
VR6	No	Peninsula Fm.

3.2 Lithological Samples

3.2.1 Thin Section Description

Thin section analysis showed that most of the sandstones had iron oxides present between quartz grains, although some at lower percentages than others (Table 3.3). Baviaanskloof samples have higher levels of feldspar and chlorite than were identified in

Goudini and Cedarberg samples. Most of the samples showed signs of fractures with iron oxides associated. Almost all of the samples had percentages of clay minerals.

Table 3.3: Mineralogy of formations determined by thin section analysis.

Formation	Mineralogy (with estimated %)	Description
Peninsula	98% Quartz 1% Clay minerals 1% Iron Oxides	Under microscope the high percentage of quartz in this sandstone is obvious. Quartz grains are large, angular and annealed together (Figure 3.4). A small amount of opaque iron oxides are apparent interspersed between the quartz grains along with clay minerals (mica) in the matrix.
Cedarberg	45% Quartz 5% Feldspar 10% Chlorite 5% Iron Oxides 35% Clay Minerals	These samples vary in grain size with some layers bordering on silt-sized grains. There are obvious layers within these thin sections. Some thin sections show fractures and s-c fabric indicating shearing (Figure 3.5). With such small grain sizes it is difficult to identify discrete minerals.
Goudini	Varied greatly: 90% Quartz 3% Iron Oxide 2% Chlorite 5% Clay Minerals	This sandstone exhibits a high quartz content but also contains small amounts of feldspar. Iron oxides are obvious in all the samples. In sample G1 there are anastomising bands of reddish iron oxides (Figure 3.6). The thin sections from rock in this formation vary greatly in the amount of iron oxide that is apparent. Iron oxides occur mainly (in samples other than G1) as opaque grains between quartz grains,

		although iron oxides also occur along fractures. These samples show a have more iron oxide than the other sandstones. The chlorite in some of the samples appears to have jagged edges.
Skurweberg	99% Quartz 0.5% Clay Minerals 0.5% Iron Oxides	The thin sections from these samples are relatively similar and all show a clean highly quartzitic sandstone. The grains tend to be large, angular and cemented together. Small amounts of iron oxide are present.
Baviaanskloof	60% Quartz 30% Feldspar 7% Clay Minerals 3% Iron Oxides	Quartz grains tend to be medium sized and angular. There is a higher sericite content in all of these samples. Iron oxides appear to occur as homogenous grains interspersed with quartz grains as well as along fractures. A lot more feldspar is also evident.
Bokkeveld	50% Quartz 5% Feldspar 5% Iron Oxides 40% Clay Minerals	There are obvious layers where the grain size varies between silt and clay sized grains. The obvious minerals are quartz and iron oxides, other minerals tend to be too small to identify.

Figure 3.4: Sample P1 in thin section showing annealed quartz grains with iron oxides between them (1cm = approximately 1mm).

Figure 3.5: Sample C3 exhibiting signs of shearing (1cm = approximately 1mm).

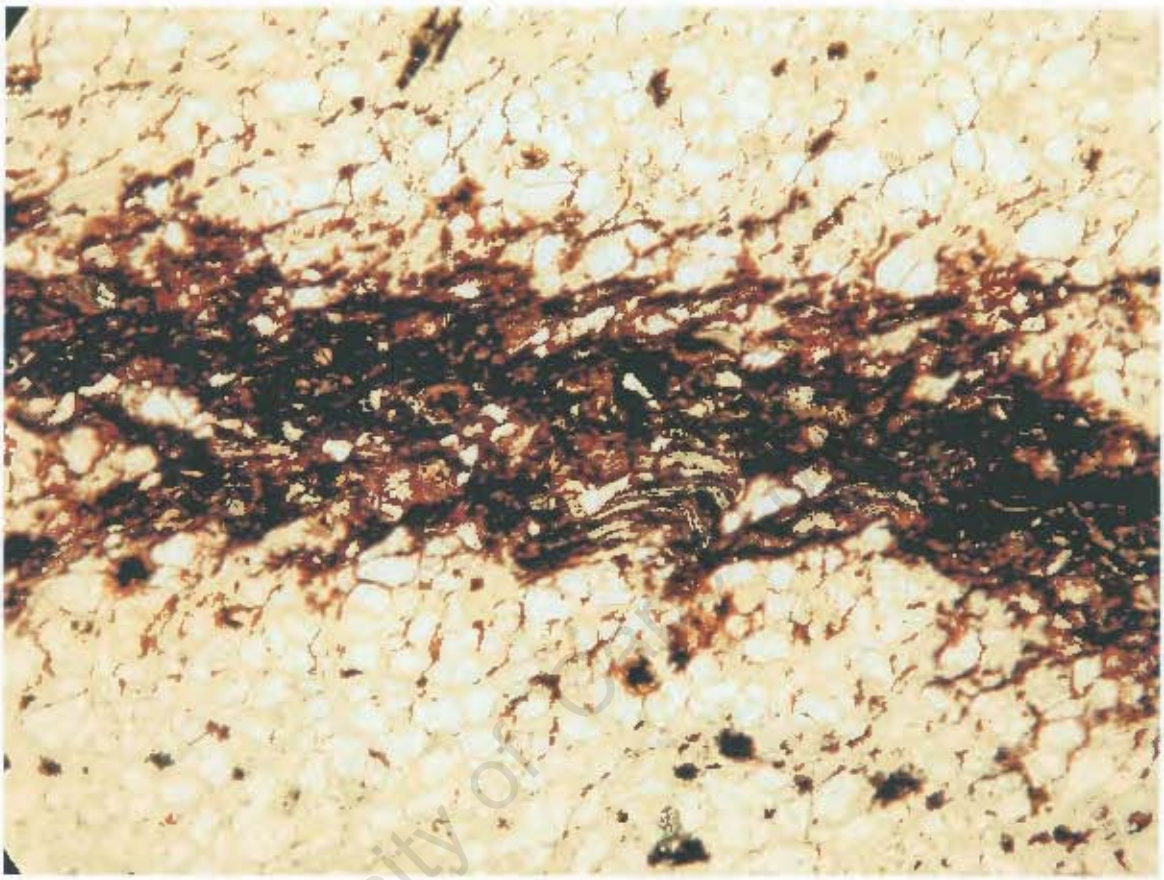

Figure 3.6: Sample G1 in thin section showing iron oxides contained within anastomising bands (1cm = approximately 1mm).

3.2.2 XRF Analysis

High levels of iron are present in the Cedarberg, Goudini and Bokkeveld Formations. The Cedarberg iron levels are consistently high whereas the Goudini iron content varies between samples (see Figure 3.7).

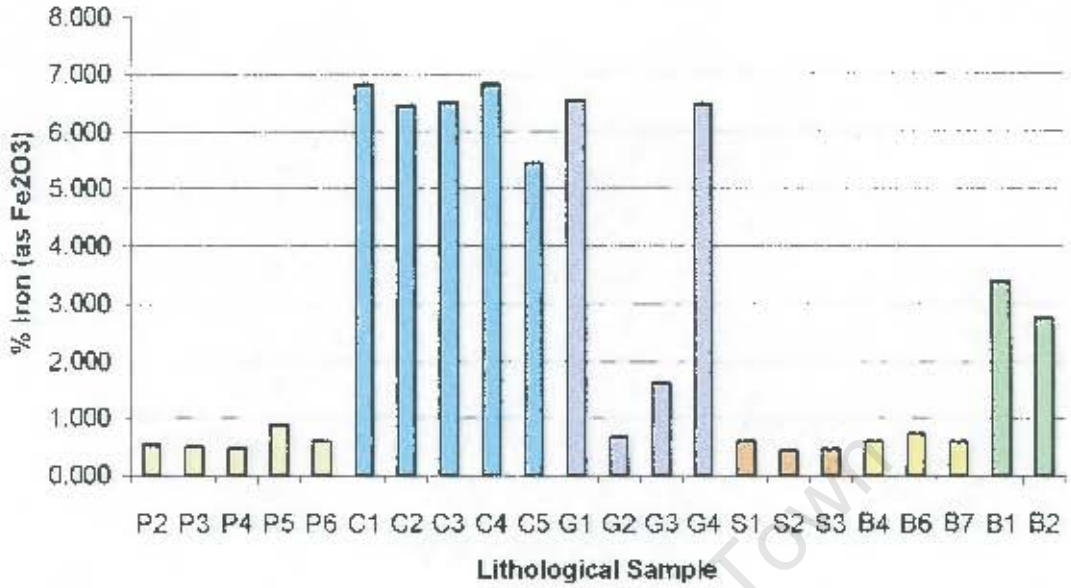

Figure 3.7: Iron percentage results of analysis of rock samples by XRF.

3.2.3 XRD Analysis

The main component of all the samples is quartz and most samples contain micas. Samples from the Cedarberg and Goudini Formations contain chlorite, possibly septechlorite. The Baviaanskloof Formation contains feldspar (both Na and K) as do the two shale Formations, the Cedarberg and the Bokkeveld. The only identified iron oxide present is haematite (see Table 3.4), however other iron oxides may be present below the detection limit (3 weight %). Goethite and ferrihydrite are amorphous and also may be difficult to pick up in XRD scans.

Table 3.4: Mineralogy indicated by XRD (see Appendix for scans).

Sample	Mineralogy from XRD, in order of peak heights.
Peninsula Fm.	Quartz, mica
Cedarberg Fm.	Quartz, feldspar, mica, haematite. 7Å chlorite peak is present without a 14Å peak, indicating a septechlorite, possibly berthierine. In some samples there is a chlorite-vermiculite peak at 13.82. Both Na and K-feldspars are present.
Goudini Fm.	Quartz, mica, chlorite, haematite
Skurweberg Fm.	Quartz, mica
Baviaanskloof Fm.	Quartz, feldspar, mica, haematite
Bokkeveld Fm.	Quartz, K-feldspars, mica, haematite

3.3 Leaching Experiments

3.3.1 Trial Leaching Experiments

Out of G1 and C2, the Goudini sample was found to leach the most iron. Variations in pH occurred over time, as did variations in iron leached (Figure 3.8). More iron was leached from both samples when organic water was used as a leachate (Figure 3.9).

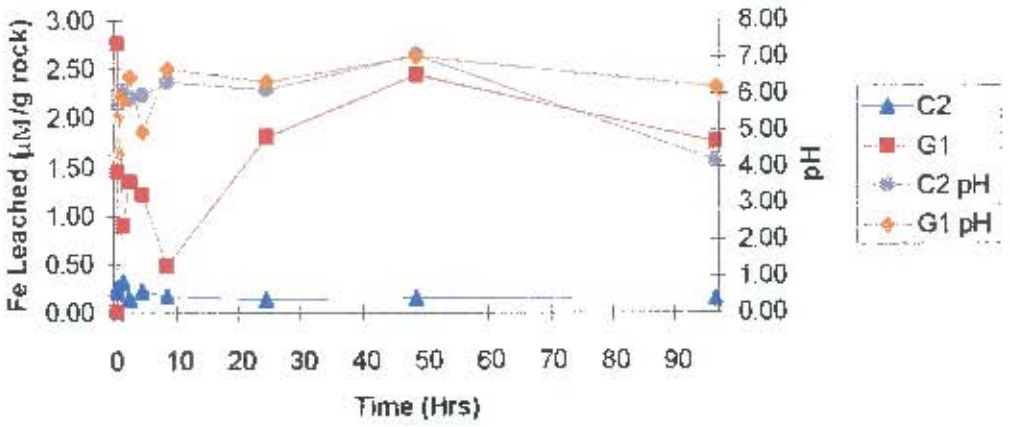

Figure 3.8: Leach of C2 and G1 using de-ionised water. Graph shows iron concentrations and pH readings in leachates through time (see Appendix for data).

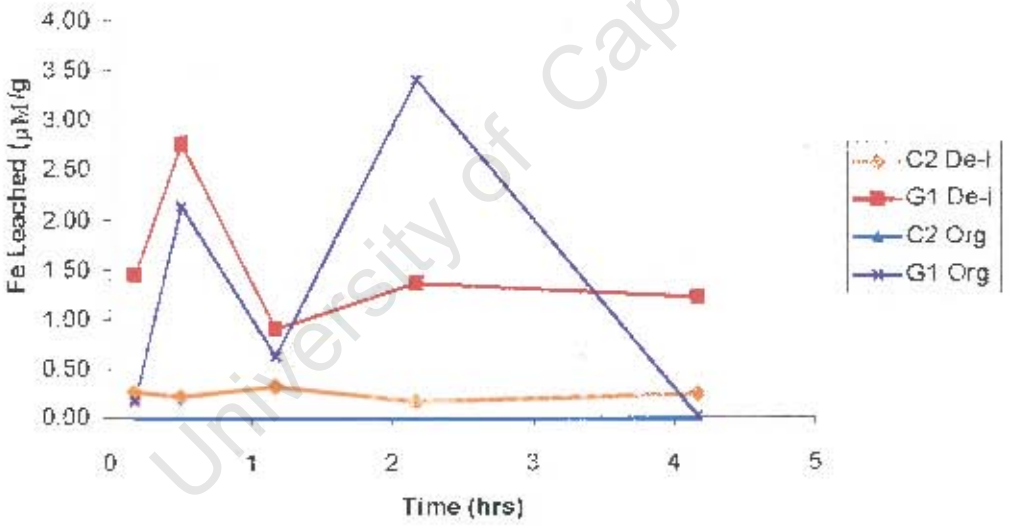

Figure 3.9: Comparison of iron concentrations measured in organic leaches and de-ionised water leaches of C2 and G1 samples (see Appendix for data). De-i = deionised water, Org = organic rich water.

The percentage of organic water in a leachate was found to affect the amount of iron leached. The general trend is that more iron is leached from samples with leachates

containing higher DOC. Pure de-ionised water (with no DOC content) however leached slightly higher amounts of iron than leachates with low DOC (see Table 3.5). Concentrations leached from C2 are so low that no trend is discernible.

Table 3.5: Amounts of iron leached for different DOC contents in leachates.

% DOC	G1 (µm iron/g rock)
100	0.38
75	0.18
50	0.15
25	0.05
0	0.15

3.3.2 Aerobic Leaching Experiments

Samples from the Goudini and Baviaanskloof Formations leached the most iron under all conditions (see Figures 3.10, 3.11 and 3.12). Most leachates showed an initial increase in iron, which then dropped off slightly and then a much larger increase in iron concentration. Towards the end of the time period iron concentrations levelled off to a plateau value. The different leachates used affected the amount of iron leached from the rock samples. Organic water buffered at pH3 generally leached the most iron (Figure 3.10), with organic water buffered at pH5 leaching less iron (Figure 3.11). Water from borehole DL17 released relatively little iron through time (Figure 3.12).

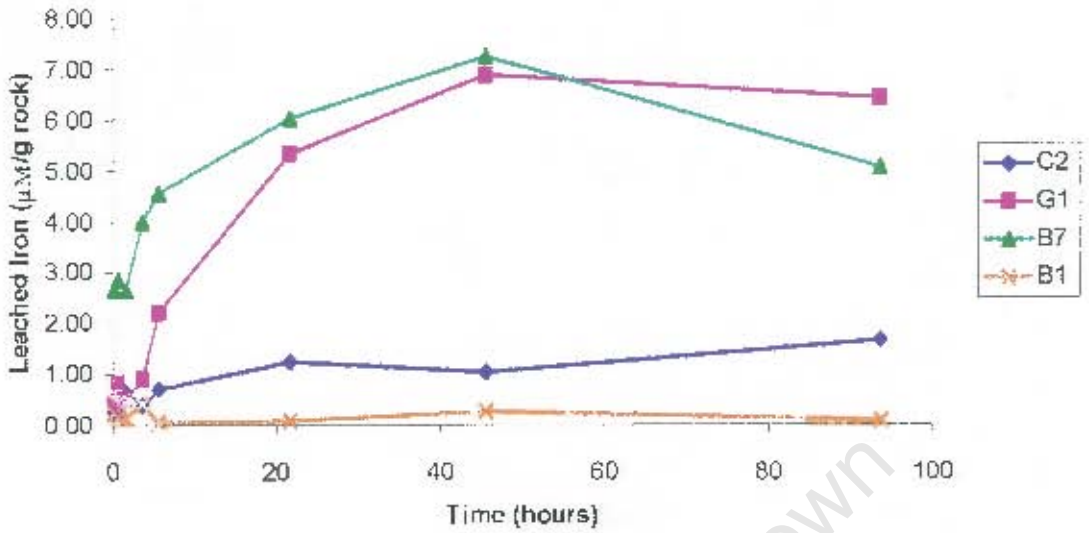

Figure 3.10: Aerobic leaching experiments on 4 rock samples using organic water buffered to pH3 (see Appendix for data).

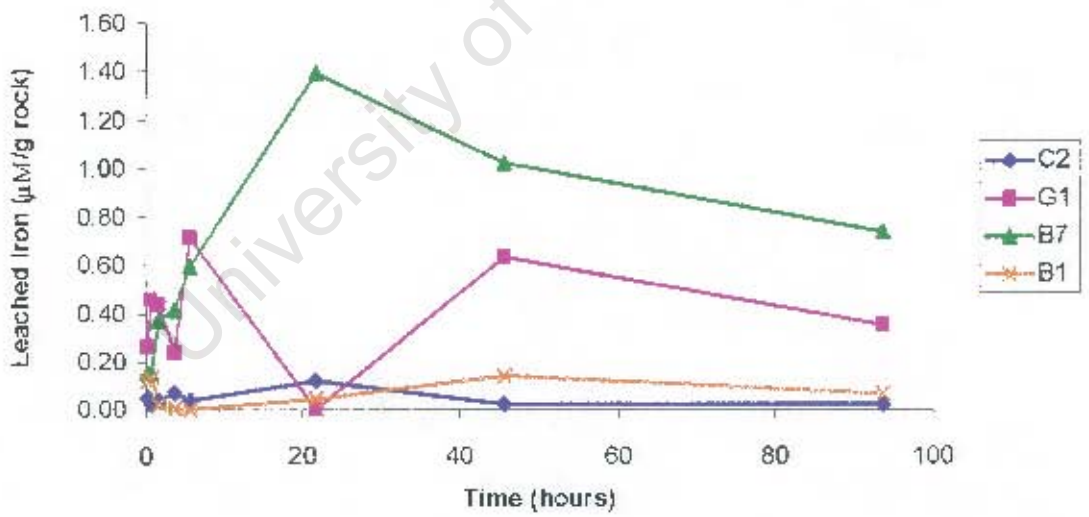

Figure 3.11: Aerobic leaching experiments on 4 rock samples using organic water buffered to pH 5 (see Appendix for data).

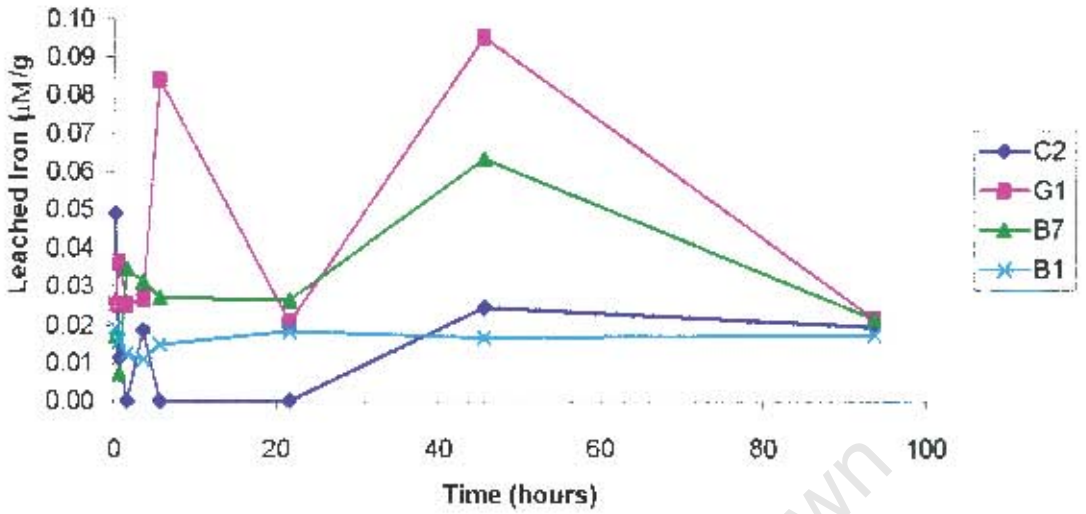

Figure 3.12: Aerobic leaching experiments on 4 rock samples using water from borehole DL17 buffered to pH 5 (see Appendix for data).

3.3.3 Anaerobic Leaching Experiments

Samples have been found to generally release more iron under anaerobic conditions. The most iron was leached from samples B7 and G1 under anaerobic conditions. The most iron was again leached by organic water buffered at pH 3 (see Table 3.6).

Table 3.6: Amount of iron leached (µm/g rock) from samples using different leachates under anaerobic conditions. nd = no data.

	P5	C2	C1	G1	B7	B4	B1	B2
MQ	0.06	0.04	0.06	1.02	4.15	1.36	0.03	0.33
DL17	0.03	0.02	0.03	2.34	5.34	1.13	0.02	1.40
pH5	0.00	0.05	1.28	4.19	11.64	14.97	0.20	1.87
pH3	2.35	2.14	0.06	9.74	14.90	nd	0.71	0.00

3.3.4 Total Reactive Iron

Samples B1 and B2 from the Bokkeveld shale have generally lower levels of total reactive iron. The sandstones (Goudini, Peninsula and Baviaanskloof) have approximately the same levels of total reactive iron and the Cedarberg samples exhibit the highest levels of total reactive iron.

Table 3.7: Total reactive iron in samples.

Sample	Total reactive iron (µm/g)
C2	65
C1	41
G1	33
G2	27
B7	35
B4	26
B1	21
B2	23
P1	9

3.4 Analytical Appraisal

ICP-MS values for particular elements tend to have a coefficient of variation of below 5%, however the coefficient of variation for iron is 48% (see Appendix). This means that the iron values measured in borehole water are less consistent than the data of other elements. Iron data from ICP-OES is more reliable as the average relative standard deviation is for each reading is lower than 2%. Leaching experiments exhibit an average coefficient of variation of 45% (see Appendix). This, although not as good as it should be, indicates that trends in the data can be reliably identified.

CHAPTER 4: DISCUSSION OF RESULTS

4.1 Mineral Sources Suggested by Water Chemistry

Iron concentrations vary greatly between boreholes suggesting that there are specific areas or lithologies that contribute to these high concentrations. Boreholes with the highest iron concentrations appear to tap into the Baviaanskloof and Goudini Formations. Both of these are probable source lithologies for elevated levels of dissolved iron in groundwater. However the data are far from conclusive; water from borehole DP29 has an extremely high iron concentration and yet the suggested source of the water is the Skurweberg Formation. There are a few possible reasons for this. Firstly, the geological coverage map is on too large a scale to accurately estimate source lithologies. Even with smaller scale maps the task would be difficult since the rocks are folded and faulted making it difficult to predict the positions of different formations at depth but no borehole logs are available. Secondly many of the boreholes are screened at a range of depths. This means that any particular borehole may have a few different lithological sources of water, e.g.: DP29 passes through Goudini Formation before reaching the Skurweberg and so some of its water may be sourced from the Goudini Formation. Thirdly iron values measured by ICP-MS show large variations between samples whereas concentrations of most other elements remain fairly constant (see Appendix). The large variations may be due to water samples not being a true reflection of aquifer water and more representative of iron behaviour in the borehole.

The pH of the water does not have an obvious relationship with the concentration of dissolved iron in the water (Figure 4.1). Generally dissolved iron in water is strongly controlled by the pH of the water (McBride, 1994). The absence of a relationship

indicates that the iron concentration is controlled by another variable, most likely pe. Miller (2000) suggests that iron concentrations in the system are controlled by a combination of pe and pH, and found that the groundwater in the Klein Karoo is poised at pe + pH = 12.

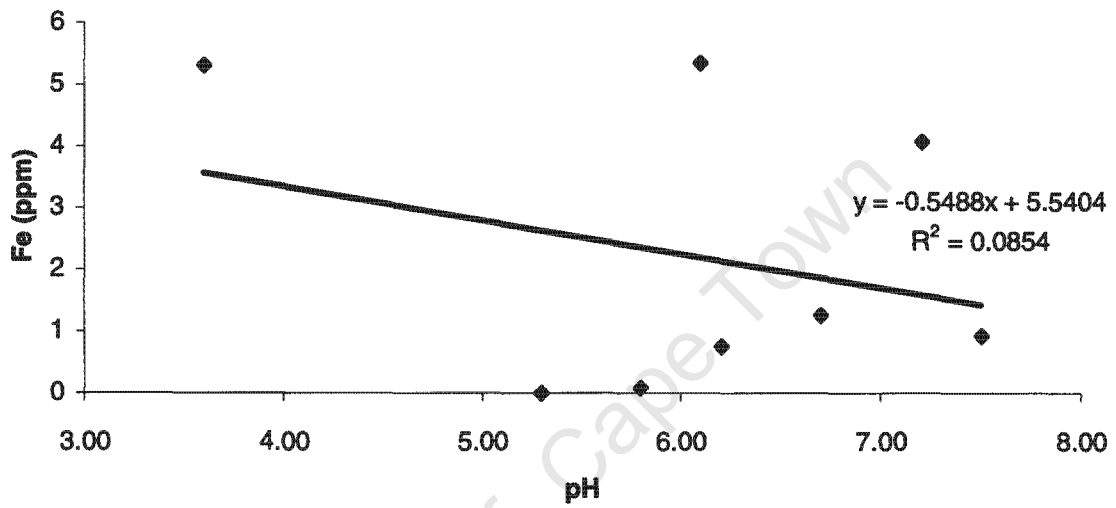

Figure 4.1: Relationship between pH and iron concentration (ICP-MS).

The correlation of iron concentrations with those of other dissolved elements may suggest possible source minerals. For example iron concentrations show an irregular but definite relationship to manganese concentrations in water samples from the boreholes (see Figure 4.2). Manganese often occurs as an inclusion in iron oxides and the dissolution of these may be the reason for its relationship with iron in the water. Another possible reason for the relationship between iron and manganese is that both occur as interlayer cations in chlorite (chemical formula: $(Mg,Fe^{2+},Fe^{3+},Mn,Al)_{12}[(Si,Al)_8O_{20}](OH)_{16}$), (Deer et al, 1992).

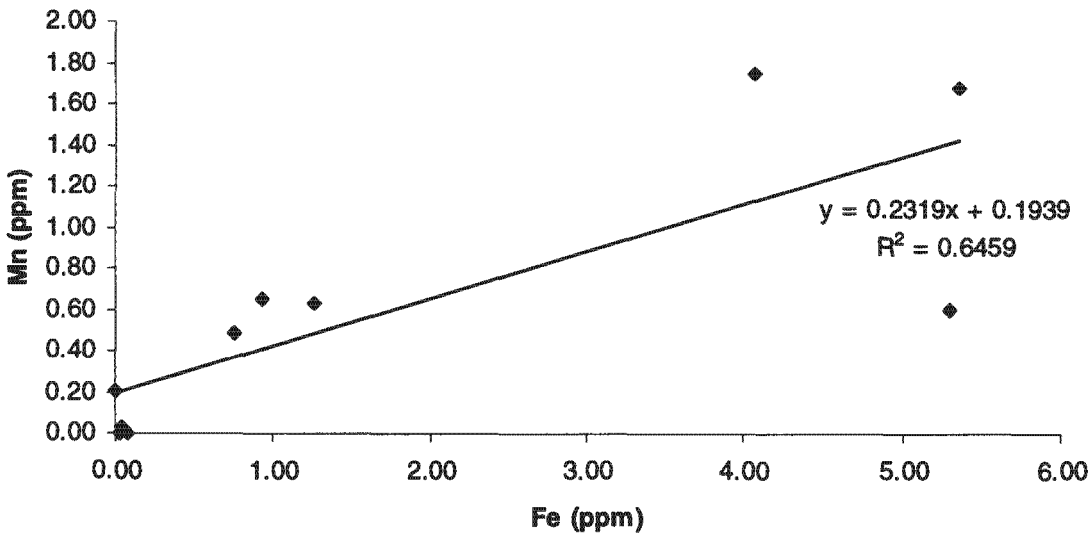

Figure 4.2: Relationship between iron and manganese concentrations in borehole water (ICP-MS).

Potassium occurs in silicate minerals such as feldspars and clay minerals but does not occur in iron oxides. The relationship between iron and potassium may be important. Iron and potassium do not correlate but there is a distinct cluster of points with low iron and low potassium and samples with higher iron concentrations also tend to have higher potassium concentrations (Figure 4.3). This may indicate that some of the iron is being dissolved from clay minerals, where it is often substituted between layers. It is likely that the water from boreholes with low iron and potassium is sourced from highly quartzitic rock with few clay minerals, such as the Peninsula and Skurweberg Formations. There are four water samples that contain persistently lower levels of all elements. These water samples are from boreholes VG3 and VR6, the artesian borehole and spring water sourced in the Skurweberg Formation. The Formations targeted by these boreholes have been roughly identified as Goudini, Peninsula and Peninsula Formations respectively. Kotze, 2000 suggests that the reason for the fresher water contained in

borehole VG3 is that it is placed on an aquizone (a portion of an aquifer with specific separate properties) where Peninsula water crosscuts the Cedarberg Formation into the Nardouw Formation. Identification of the actual source formations of these boreholes will aid in further borehole placement.

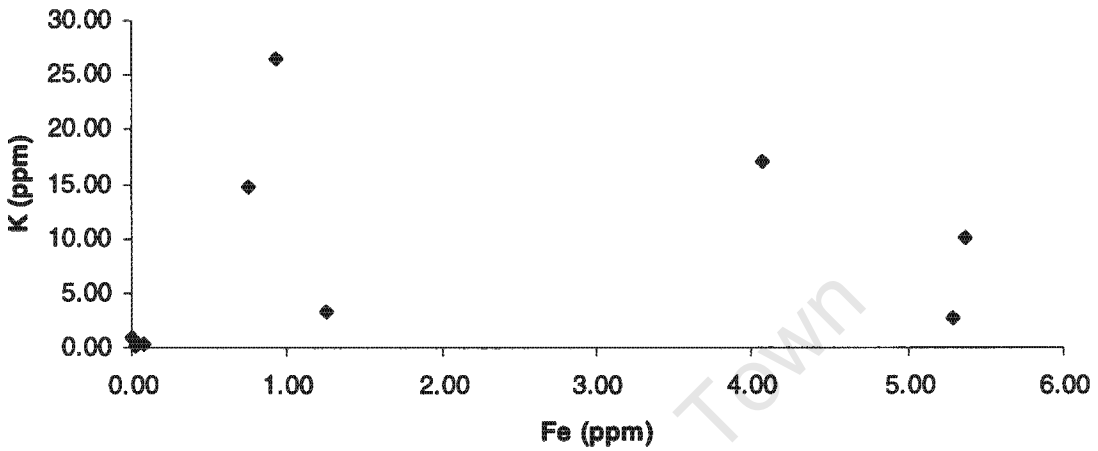

Figure 4.3: Relationship between potassium and iron in borehole water (ICP-MS)

If iron is being weathered from iron sulphides a relationship between iron and other chalcophile elements such as arsenic and nickel would be expected. There is no obvious relationship between iron and arsenic but nickel occurs in higher concentrations with higher concentrations of iron. Therefore it is possible that iron is being weathered from iron sulphides such as pyrite but it is unlikely that these are the only source of iron.

4.2 Available Iron Containing Minerals in TMG Rocks

Iron can occur in sedimentary rocks in three ways. Firstly iron-containing minerals can be originally deposited with the formation as a primary mineral e.g.: magnetite, ilmenite. Secondly, iron-containing minerals can be precipitated from porewater during diagenesis

e.g.: chlorite. Thirdly, iron can be remobilised from its original form (as either a primary or diagenetic mineral) and re-precipitate in fractures as iron oxides. All the formations contain at least small amounts of iron oxide minerals.

Many of the sandstones have annealed quartz grains indicating that they were highly compressed during diagenesis. This evidence supports what the literature says about the sandstones being well indurated with little or no primary hydraulic connectivity (Kotze, 2000). As mentioned in the introduction the hydraulic connectivity arises from microscale fractures, which are evident in thin sections (Rosewarne, 2002). The samples containing fractures and some Cedarberg samples showing s-c fabrics were collected from near to fracture zones. Fractures in particular show high levels of iron oxides but there are iron-oxide minerals as small grains within the matrix as well.

The iron oxides from all the samples were identified as being haematite (Fe_2O_3), which contains iron in the Fe^{3+} form (Cornell & Schwertmann, 1996). This means that the iron present in the samples would have to be reduced to Fe^{2+} before it could be released in its dissolved form into the water. This reduction may take place under anoxic conditions in the aquifer with the help of iron reducing bacteria (Straub *et al.*, 2001). No attempt was made in this project to simulate leaching conditions with bacteria present. However no attempt was made to sterilise any of the samples either. The reduction of ferrous iron by iron-reducing bacteria and their role in the leaching of iron from rock would be an interesting avenue for further research.

In sample G1, iron oxides occur predominantly within anastomising bands, implying that iron occurs in distinct zones within the formation. This banding was only evident at one site in the field. XRF data supports this as it shows that samples from the Goudini have

large variations in iron content. A potential explanation for the huge variation in iron is the exchange of porewaters between formations during diagenesis. Porewater trapped in sediments can become overpressured following the rapid burial of sediments and remain in place. In clayey units (such as the Cedarberg) overpressure may be extremely common. Porewaters normally evolve in place by sediment-water interactions but when pressure is released they will flow up through overlying sediments. When flowing through these sediments, the porewaters can leave mineralogical signs of their presence (de Caritat & Baker, 1992). This exchange could have occurred between the Cedarberg Formation and parts of the immediately overlying Goudini Formation, thus causing variations in the mineralogical content of the Goudini Formation. The Cedarberg Formation has a high percentage of iron therefore porewaters from that formation could have carried iron to parts of the Goudini Formation.

A common iron containing diagenetic mineral occurring in the sediments is chlorite. Chlorite may contain iron and so is also a possible source of iron. Chlorite was found (by XRD and thin section analysis) in sample G1, all the Cedarberg samples and a small signal was present in the Bokkeveld samples. All of these samples have relatively high levels of iron when analysed by XRF suggesting that chlorite is a source of the iron. Chlorite is a layered structure that resembles the micas and its general formula is $(Mg,Fe^{2+},Fe^{3+},Mn,Al)_{12}[(Si,Al)_8O_{20}](OH)_{16}$ (Deer et al, 1992). Berthierine, a particular iron rich septachlorite mineral that often occurs in iron rich sedimentary rocks was identified, by the absence of the characteristic 14Å chlorite peak and presence of a 7Å peak. Chlorite is a diagenetic mineral that tends to be unstable under low pH weathering conditions and when chlorite minerals weather a preferential release of the octahedrally co-ordinated cations (such as iron manganese and aluminium) occurs. This may explain the presence of secondary iron oxides in some of the samples since they could have

been formed from iron weathered from the chlorite. After the loss of the octahedrally co-ordinated cations the chlorite tends to transform into alternating chlorite-vermiculite layers (Brandt et al, 2002). A few of the samples containing chlorite also had XRD peaks at 13.8 Å indicating the chlorite-vermiculite weathering product of chlorite. This means that the chlorite (at least in some of the samples) is weathering to release cations and therefore may be a possible source of iron released into the water. The weathering of chlorite to iron is evident in thin section along the weathered edges of the rocks. It is difficult to determine whether the iron minerals within the matrix are primary or diagenetic, but chlorite is diagenetic and a possible source of iron (de Caritat & Baker, 1992).

Some samples in the Peninsula Formation showed what seemed to be a release of pressure towards the weathered edges. This was revealed as hairline cracks parallel to the edge of the rock that contained more iron oxides than the rest of the sample (see Figure 4.4). The iron oxides may have been deposited there from elsewhere as the sample was weathered, or they may be a product from the weathering of minerals in the Peninsula Formation. In this case it is suggested that the chlorite in the fresh part of the sample has been weathered to vermiculite and iron oxides towards the weathered edges, thus iron is being mobilised from the weathering of chlorite.

Figure 4.4: Change in sample P1 towards its weathered edge, on the right of the photograph (1cm = approximately 1mm)

Although samples with high levels of iron under XRF also contain chlorite, sample G4 seems to be the exception. Little iron was visible in samples G4 in thin section and yet XRF analysis shows it to contain relatively high levels of iron. In thin section G4 is composed of annealed quartz grains. The quartz grains appear to contain inclusions and the high iron percentages may be due to the iron being included in the quartz grains. Inclusion can occur when a sandstone is put under high pressure. The pressure differences may cause specific conditions that are enough to put quartz into solution. The quartz would then migrate and precipitate in the pore spaces. Any minerals already present in the pore spaces would become included into the quartz when re-precipitation occurs (Hutcheon, 1990). This is likely to be what happened to sample G4 since it was sampled near to a fault.

There is a difference in the type of feldspars present in the different shales. The Cedarberg Shale contains both Na and K-feldspars, yet the Bokkeveld only contains K-feldspars. Using Bowen's reaction series K-feldspars are more resistant to weathering than Na-feldspars and so can indicate that the Bokkeveld samples are more highly weathered (Battey, 1981). In this case the difference in weathering is unlikely since some of the Cedarberg samples were highly weathering. The difference in the feldspars therefore probably indicates a difference in the source area of each of these sediments. The Bokkeveld formation also contained lower levels of iron and so may be from a different source area that is rich in potassium but deficient on iron.

Iron and potassium show a basic correlation since when the percentage of potassium in a sample is high, the iron percentage is also high (see Figure 4.5). Potassium indicates the presence of clay minerals and feldspars. The fact that iron percentages are higher in samples with higher potassium indicates that at least some of the iron is probably associated with clay minerals (it is unlikely to associate with feldspars). Samples from different lithologies show specific correlations between potassium and iron. The Skurweberg and Peninsula Formations are clustered together and exhibit both low iron and potassium percentages, confirming the low clay content noted in thin section. As expected, the Cedarberg shale has high potassium and this is strongly associated with high iron. The clay minerals in the Cedarberg Formation therefore contain high levels of iron. The Bokkeveld shale on the other hand also exhibits high percentages of potassium but lower percentages of iron. The lower percentage of iron may be due to the clay minerals in the Bokkeveld shale containing less iron or the presence of more K-feldspars. The Goudini Formation, as seems to be characteristic, is highly variable with one sample falling in the same range as the Cedarberg Formation and another in the

cluster containing Peninsula and Skurweberg samples. This high level of variability means that the Goudini formation contains varying amounts of clay minerals and feldspars. The Baviaanskloof Formation samples show high percentages of potassium with lower percentages of iron, indicating that most of the potassium is due to feldspars or clay minerals deficient in iron. Since feldspars were identified in thin section it is likely that most of the potassium occurs in feldspars in the Baviaanskloof Formation.

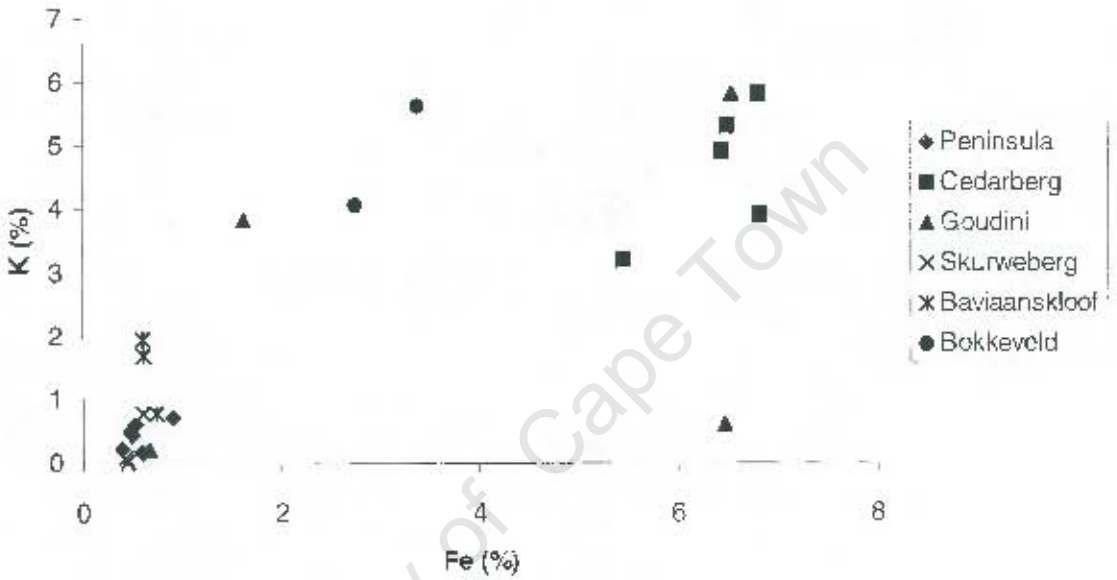

Figure 4.5: Relationship between iron and potassium (XRF).

Iron and manganese also show a basic correlation- with higher percentages of iron being related to higher percentage of manganese (Figure 4.6). Manganese often occurs as an inclusion in iron oxides as well as alongside iron in chlorite. The Goudini Formation again shows the largest variation in sample composition with the three samples falling into groups with the Cedarberg, Bokkeveld Peninsula and Skurweberg Formations. The fact that G1, the Goudini sample with the highest iron percentage, falls into the same region as samples from the Cedarberg Formation may suggest similarities

in the chemistry of the samples. This reinforces the above suggestion that an exchange of porewaters may occur between some parts of the formations during diagenesis.

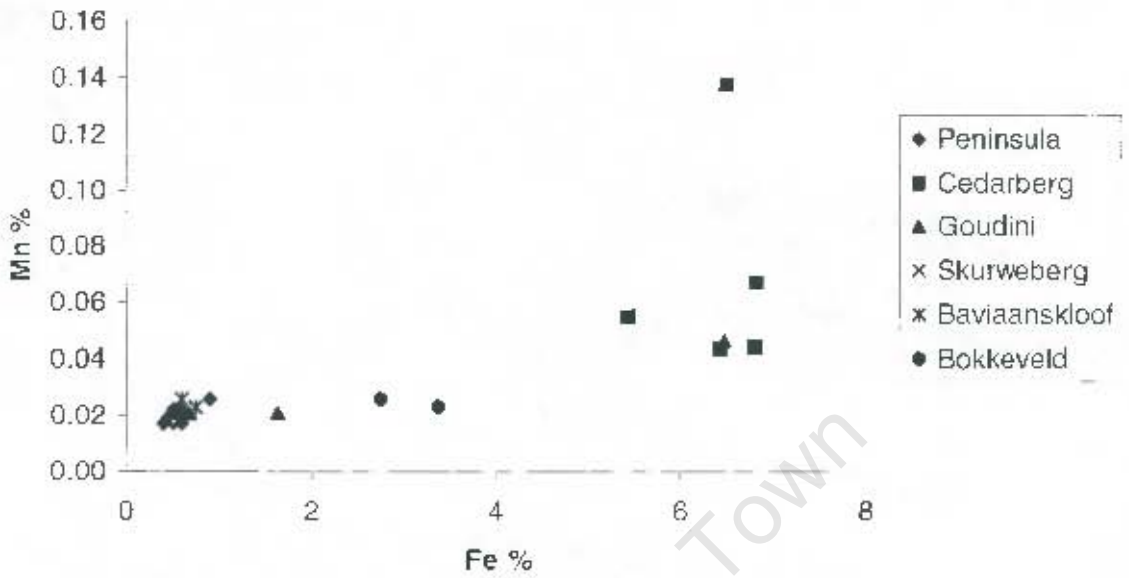

Figure 4.6: Relationship between iron and manganese (XRF)

4.3 Leachability of Iron

The presence of iron in rocks is irrelevant to groundwater unless that iron is available in solution. Initial leach tests on samples G1 and C2 indicate that there is not a straightforward leaching process occurring. Levels of iron vary greatly through time and not with any particular trend. The variations may be due to iron being leached from the sample and then being readsorbed onto the surface of the powder or re-precipitated in a different form. The pH varied greatly over time as well and this is possibly due to the large surface area of the powdered samples offering many sites on which H^+ ions were able to bind. The variations in pH would also have affected the dissolution and readsorption of iron.

Powdered samples were used in the leach tests in order to increase reaction and leach rates so gaining results over a shorter period of time. The use of powdered sample may have, however, affected leach results, as with so much surface area available it was favourable for iron to be readsorbed onto the powdered sample. This may have resulted in an inaccurate portrayal of the leaching of iron through time. Nevertheless the leaching of the samples through time relative to each other was the main aim of this research and this should not have been affected.

4.3.1 Effect of pH

The pH of water from the aquifer varies greatly from as low as 3.6 up to 7.4 (see Appendix). As mentioned above the pH of the water should have a significant affect on both the rate and extent of dissolution (and therefore the leaching) of iron. Two different pHs were chosen for the leaching experiments in order to closely simulate conditions within the aquifer. A pH of 5 would more closely simulate the average conditions in most of the aquifer. The pH of 3 was expected to give a faster reaction due to the lower pH (since iron is more soluble at lower pH) and although it may seem extreme it is still within the parameters of the aquifer. Organic buffers were used to keep samples at these pHs so as to simulate natural conditions as closely as possible.

The pH greatly affected the extent of leaching from all the samples and samples at pH 3 leached far more iron than samples at pH 5 (see Figure 4.7). Water in the aquifer has, in some cases a low pH and these conditions, although not as extreme as water at pH 3, may exacerbate the weathering of iron from the rocks.

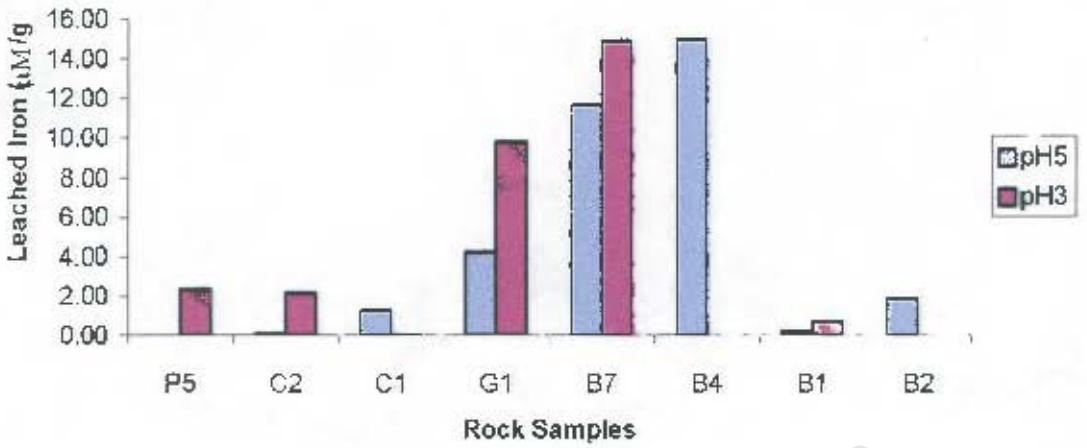

Figure 4.7: A comparison between samples leached under anaerobic conditions with an organic water leachate of pH 3 and an organic water leachate of pH5 (see Appendix for data). Notice there is no data point for sample B4 at pH 3 because it was lost.

4.3.2 Effect of DOC

It was expected that the use of organic rich water would speed up the leaching of iron from the rock samples and increase the amount of iron leached. The mechanism suggested for this is that organic molecules act as ligands and attach themselves to iron in a rock sample. The iron therefore becomes dissolved along with the organic molecule. As reduction occurs the organic molecules are broken down until, in an anoxic environment, the iron is released (Heyes & Moore, 1992). The organic ligands not only speed up the reaction but also closely simulate what may be happening to the water as it enters into the aquifer. The water would pass through organic rich soils and enter into the aquifer where iron would be chelated: reduction would then take place liberating the iron under anaerobic conditions. When a borehole is drilled into the system it becomes oxic and the iron precipitates in the oxidised form. The results

comparing the use of organic rich water with non-organic water do show that organics increase the amount of iron that is leached from a sample (see Figure 4.8).

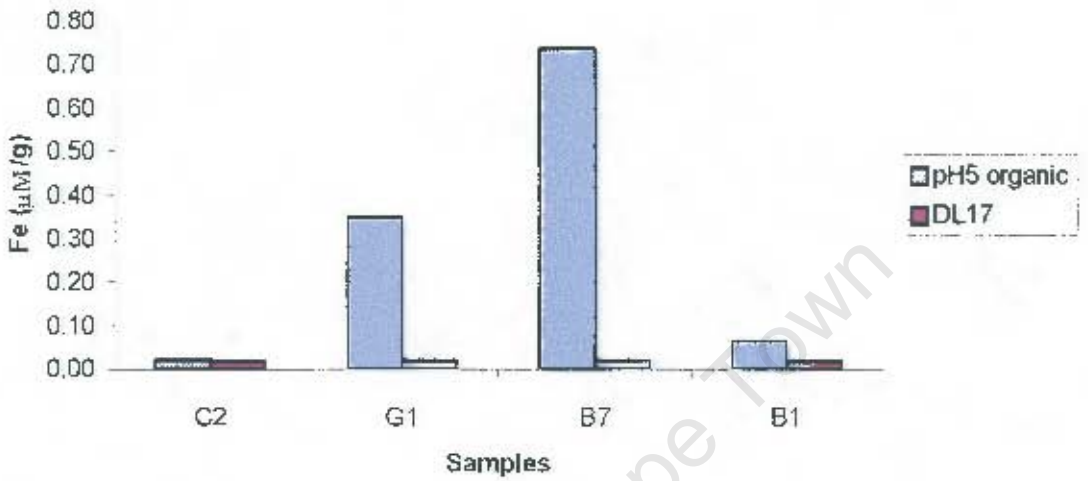

Figure 4.8: Comparison between samples leached under aerobic conditions at pH 5 by organic-rich water and organic deficient water (DL17).

It has been found that large increases in DOC do not bring the same magnitude of iron leachability, due possibly to the limits on surface reactions (Heyes & Moore, 1992). This means that even a small amount of DOC in the water may increase the leachability of iron greatly.

Heyes and Moore (1992), suggest that dissolved organic carbon (DOC) may be adsorbed onto the surface of the sediments or co-precipitate with Fe, Ca or Mg. The occurrence of precipitation or adsorption may have caused some inaccuracies in the data since the sediments along with any precipitates would have been filtered out. It was also found that some DOC was lost when the organic water was passed through a

0.45µm filter. In the aerobic and anaerobic leaching experiments 0.2µm filters were used. If any iron were still complexed to the organic water it would be filtered out as well thus causing inaccuracies in the results. This is unfortunate but cannot be helped since 0.45µm filters were found to be allowing colloidal iron through which was not desirable. However it has been found that 90% of the dissolved organic carbon (DOC) that passed through a 1.2µm filter also passed through a 0.1µm filter, so the analytical effect of using smaller filter sizes may be negligible (Heyes & Moore, 1992). The iron concentration in organic water could not be used as a blank for samples leached with organic water as it was found that some leachates had lower concentrations of iron than the organic water. This may be due to the iron from the organic water being adsorbed onto the surface of the crushed rock during leaching.

4.3.3 Aerobic and Anaerobic Conditions

Anaerobic conditions proved to aid in the leaching of iron from the rock samples, with values of iron much higher under anaerobic conditions (see Figures 4.9, 4.10 and 4.11). The waters of the TMG have a measured DO content of 0mg/L (Smith pers comm., 2003). This value differs from values found in this research due to the difference in methods employed. Cavé and Smith took *in situ* measurements using a down-hole log (Cavé & Smith, 2004) whereas this research used water pumped from a borehole, which means that the water will already to some extent have equilibrated with the atmosphere. The difference between aerobic and anaerobic conditions is more exaggerated in DL17 leachate where there is less DOC. Heyes and Moore (1992), suggest that DOC is less effective as a weathering agent under anaerobic conditions even though DOC sorption onto the surface of the sediment is lowered. And indeed the fact that DOC is less likely

to sorb to the surface of a sample may mean that it is less likely to bond to cations in a mineral and remove them.

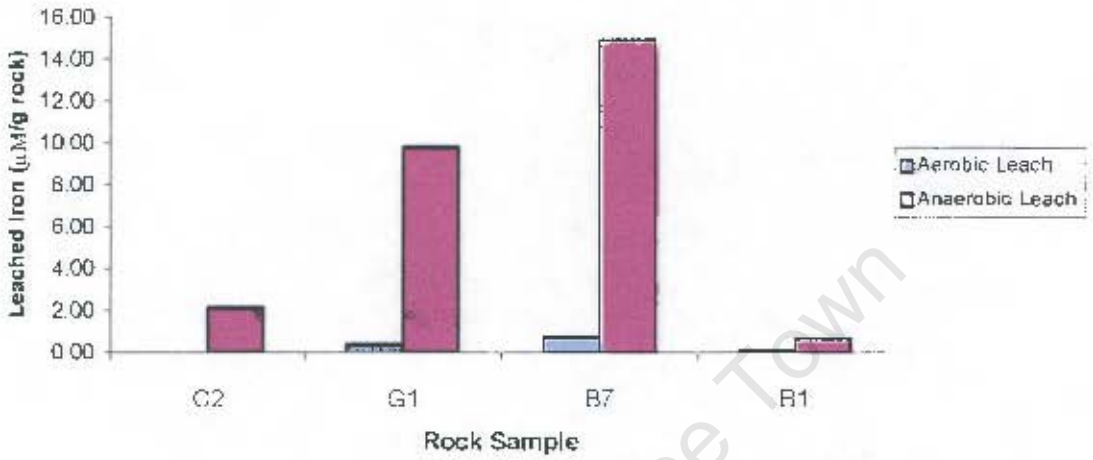

Figure 4.9: A comparison between samples leached using organic water buffered at pH3 under aerobic and anaerobic conditions (see Appendix for data).

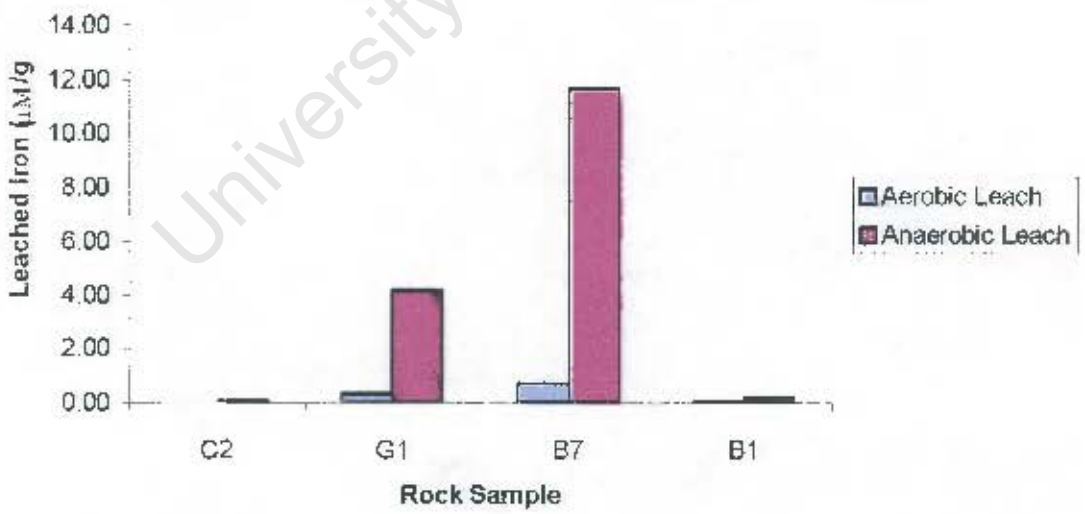

Figure 4.10: A comparison between samples leached using organic water buffered at pH5 under aerobic and anaerobic conditions (see Appendix for data).

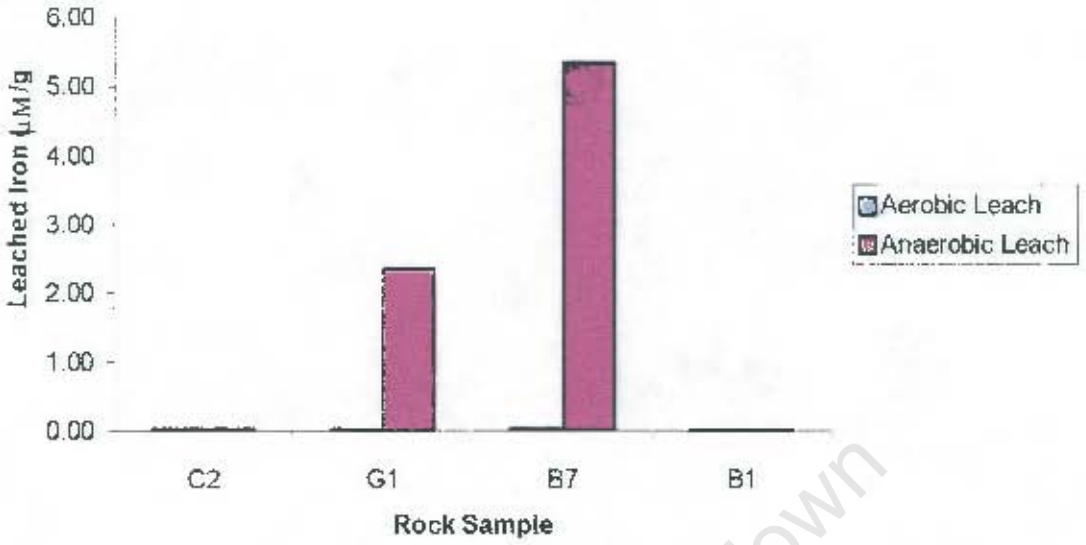

Figure 4.11: A comparison between samples leached using water from borehole DL17 buffered at pH5 under aerobic and anaerobic conditions (see Appendix for data).

The leaching of iron through time seems to follow a trend under aerobic conditions (see Figures 3.8, 3.9, 3.10, 3.11 and 3.12). There appears to be an initial release of iron which then tapers down and then another (larger) release of iron, which tapers off slowly towards the end of the time series. The initial release of iron may be due to either exchangeable or sorbed iron being released or the more easily leached iron oxides being dissolved. Once this occurs the iron is re-adsorbed onto the surface of the crushed rock or precipitated. The second rise in dissolved iron may be due to the release of more tightly bound iron either in mineral form (clay minerals, chlorite) or iron oxides. The data of Heyes and Moore (1992), which are from similar leaching experiments, also show this trend although it was not commented on. All of the aerobic graphs show this trend and further investigations should be carried out to determine the mechanisms controlling the trend.

4.3.4 Percentage of Total Iron Leached

The percentage of total iron leached from all the samples is low (see Figure 4.12). This means that very little of the available iron is actually being leached even under extreme conditions such as using organic leachates buffered at pH3. Most of the iron is therefore not available to be leached during the time of the experiments. However under aquifer conditions the rocks and water are in contact for long periods of time and weathering can be allowed to occur to a greater extent and more iron can become available for dissolution.

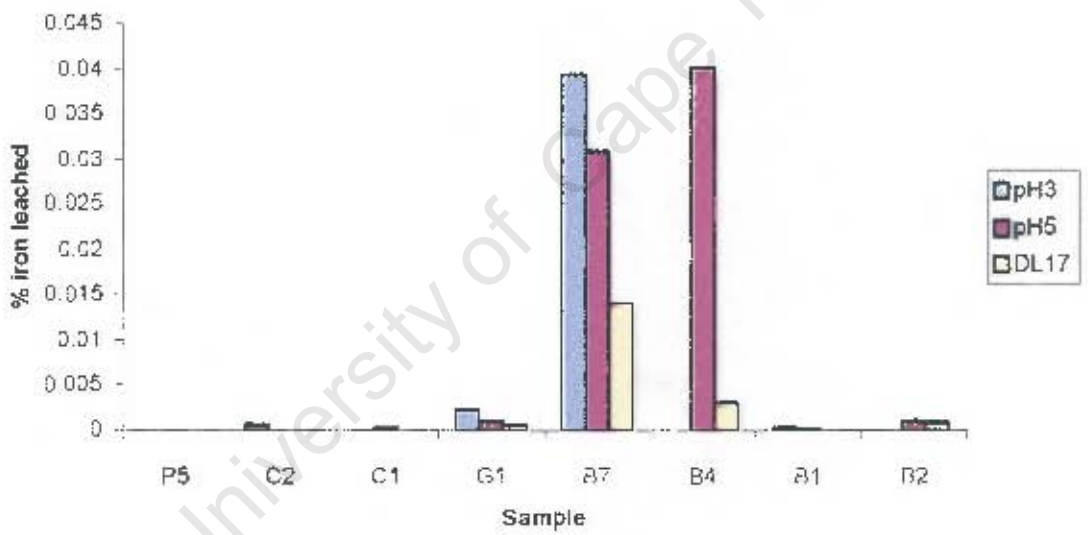

Figure 4.12: The percentage of total iron leached under anaerobic conditions.

The Baviaanskloof Formation showed relatively low percentages of iron under XRF and yet surprisingly leached as much iron as G1. The percentage of total iron leached is therefore much higher in the Baviaanskloof samples than the other samples. This may be due to the iron in the Baviaanskloof Formation being more available either because it

is in a different mineralogical form (such as more easily leached iron oxides) or because the samples were more highly weathered.

Total reactive iron gives an indication of the amount of iron oxides present in a sample. In sandstone samples from the Peninsula, Baviaanskloof and Skurweberg Formations the total reactive iron is close in value to the total amount of iron indicating that most of the iron in these samples is present as iron oxides. The Bokkeveld samples have relatively low amounts of total reactive iron, meaning that most of the iron in the samples exists in a form other than iron oxides. From the XRD scans the iron is most likely contained in iron oxides. The Cedarberg samples have the highest levels of total reactive iron, however these are only a small part of the total iron in the samples. The Cedarberg samples therefore have high amounts of iron oxides, but also high amounts of iron in another form. Sample G2 falls into the same category as the Peninsula, Skurweberg and Baviaanskloof samples yet sample G1 has similar results to samples from the Cedarberg, indicating again that a lot of the iron exists in a form other than iron oxides. Sample G1 has less iron contained in iron oxides and more in other forms than the Cedarberg samples since it has lower total reactive iron values. It is probable that the iron is contained in clay minerals, particularly chlorite in samples from the Cedarberg and Bokkeveld as well as sample G1. Yet again sample G1 shows a similarity to the Cedarberg samples reinforcing the likelihood of an exchange of porewater during diagenesis. It appears that iron oxides tend to be more easily leached from rock samples over the short period of the leaching experiments, longer leaching experiments may be able to determine leaching of iron from other mineralogical sources such as chlorite.

CHAPTER 5: CONCLUSIONS AND RECOMMENDATIONS

There is no simple answer to the lithological source of iron in the TMG. Samples with high percentage composition of iron do not necessarily indicate that that iron is available for dissolution in the groundwater. Comparing the stratigraphy of boreholes to the historical incidence of clogging indicates that the Goudini and Baviaanskloof are the most likely source aquifers for those boreholes with iron clogging problems. It can therefore be inferred from this data that the iron is sourced in these formations.

There are relatively high percentages of iron in the Cedarberg and Bokkeveld Formations as well as some samples from the Goudini Formation, suggesting that these formations are possible sources of iron. The iron tends to be in the form of iron oxides and clay minerals, specifically chlorite. As the chlorite weathers the iron is released and precipitates between quartz grains as iron oxides, specifically haematite.

Iron is most easily leached from some samples from the Goudini and Baviaanskloof Formation. The amount of iron released over the period of time that the experiments were run was also higher than other samples. This indicates that the Baviaanskloof and Goudini Formations are likely sources of iron in the groundwater.

The Goudini Formation showed variation in the amount of iron contained in different samples as well as the leaching of that iron. It is likely that parts of the Goudini Formation were involved in an exchange of porewaters with the Cedarberg Formation during diagenesis, which affected their chemistry. Some parts of the Goudini Formation may be richer in iron than others.

Iron is most easily leached from the rock samples in an anaerobic low pH environment with at least small amounts of DOC available. It is suggested that the organic content enters the water as it percolates through the soil and then aids in the dissolution of iron from the rocks as the water enters the aquifer. Since water in the aquifer is under anaerobic conditions more iron is likely to dissolve in it and remain in solution until the water becomes oxidising again- in a borehole. The relatively low pH waters in the aquifer will also aid in the dissolution of iron from the rocks.

The leaching experiments were run over a short period of time, not long enough to simulate what is actually happening in the aquifer, however all the data indicates that part of the Goudini and Baviaanskloof Formations are the sources of iron in the groundwater in the Kammanassie Mountains area.

Recommendations for further research:

- An investigation into the variations in chemistry (specifically iron content) of the Goudini Formation.
- Chemical analysis of chlorite occurring in the TMG rocks particularly looking at its iron content.
- A thorough determination of the stratigraphy of boreholes in the area, specifically relating to those experiencing iron clogging problems.
- More thorough investigation of the leaching of iron from rocks in the TMG involving leaching over a longer period of time to more closely simulate aquifer conditions.
- An investigation into the role of iron reducing bacteria in the dissolution of iron from rocks in the TMG.

REFERENCES

Bain, D.; 1976; The weathering of ferruginous chlorite in a podzol from Argyllshire, Scotland; *Geoderma*, **17**, pp193-208

Brandt, F.; Bosbach, D.; Krawcyk-Bärsch, E.; Arnold, T.; Bernhard, G.; 2002; Chlorite dissolution in the acid pH-range: A combined microscopic and macroscopic approach; *Geochimica et Cosmochimica Acta*, **67**, pp1451-1461

Cape Nature Conservation; 2003; Kammanassie Nature Reserve; www.capenature.org.za/nature_reserves/html/kammanassie.html

Cavé, L.; 2002; *Apophyllite weathering and the aqueous geochemistry of a Karoo breccia pipe;* Unpublished PhD Thesis, University of Cape Town, Cape Town

Cavé, L.C.; Smith, M.E.; 2004; *In-borehole measurements of chemical parameters in a wellfield affected by iron biofouling*; In: Wanty, R.B.; Seal, R.R.; II (eds); Water Rock Interaction, Volume 2: Procedings of the 11th International Symposium on WRI, Saratoga Springs, New York, USA, 27 June- 2 July 2004. AA Balkema, Leiden. p.1179-1184.

de Caritat, P.; Baker, J.; 1992; Overpressure release, cross-formational porewater flow and diagenesis; in Kharaka, Y.; Maest, A.; *Water Rock Interaction (Volume 2: Moderate and high temperature environments)*, A.A. Balkema, Netherlands.

Deer, W.; Howie, R.; Zussman, J.; 1992; *An introduction to the rock forming minerals* (ed 2); Longman Scientific and Technical, England

de Beer, C.; 2002; The Stratigraphy, lithology and structure of the Table Mountain Group; *A synthesis of the Hydrogeology of The Table Mountain Group- Formation of a research strategy*; Water Research Commission, South Africa; WRC report number TT 158/01

Drever, J.; 1997; *Geochemistry of natural waters – Surface and groundwater environments* (ed 3); Prentice Hall Inc., USA

Hartnady, C.; Hay, E.; 2002; Potential of TMG aquifers and integration into catchment water management; *A synthesis of the Hydrogeology of The Table Mountain Group- Formation of a research strategy*; Water Research Commission, South Africa; WRC report number TT 158/01

Heyes, A.; Moore, T.; 1992; The influence of dissolved organic carbon and anaerobic conditions on mineral weathering; *Soil Science* **154**, pp 226-236.

Hutcheon, I.; 1990; Aspects of the diagenesis of coarse-grained siliclastic rocks; in McIlreath, I.; Morrow, D.; *Diagenesis*; The Runge Press Ltd., Canada.

Jolly, J.; 2000; Biofouling in boreholes of the Klein Karoo Rural Water Supply Scheme, Oudtshoorn, South Africa, and their effect on well scheme management; *Groundwater: Past achievements and future challenges*; Sililo et al.; Rotterdam

Jolly, J.; Engelbrecht, P.; 2001; Biofouling in boreholes of the Klein Karoo Rural Water Supply Scheme, Oudtshoorn (South Africa) and the effect on well scheme management; *Borehole Water Journal* **49**, pp15-17.

Jolly, J.; Engelbrecht, P.; 2002; Occurrence and management of iron related borehole clogging in Table Mountain Group aquifers; *A synthesis of the Hydrogeology of The Table Mountain Group- Formation of a research strategy*; Water Research Commission, South Africa; WRC report number TT 158/01

Jolly, J.; Kotze. J.; 2002; The Klein Karoo Rural Water Supply Scheme; *A synthesis of the Hydrogeology of The Table Mountain Group- Formation of a research strategy*; Water Research Commission, South Africa; WRC report number TT 158/01

Kasrils, R.; 2002; Preface in: *A synthesis of the Hydrogeology of The Table Mountain Group- Formation of a research strategy*; Water Research Commission, South Africa; WRC report number TT 158/01

Kotze, J.; 2000; *Hydrogeology of The Table Mountain Sandstone Aquifer- Klein Karoo*; Unpublished PhD Thesis, University of the Free State, Bloemfontein

Kotze, J.; Rosewarne, P.; 1999; *Klein Karoo Rural Water Supply Scheme augmentation study*; Commissioned by the Department of Water Affairs and Forestry: SRK Consulting

Mackintosh, G.; de Villiers, H.; 2002; Treatment of soft, acidic and ferruginous groundwaters; *A synthesis of the Hydrogeology of The Table Mountain Group- Formation of a research strategy*; Water Research Commission, South Africa; WRC report number TT 158/01

McBride, M.B.; 1994; *Environmental Chemistry of Soils*, Oxford University Press, New York

Meyer, P.; 1999; *An explanation of the 1:500 000 general hydrogeological map, Oudtshoorn 3320*; Department of Water Affairs and Forestry, South Africa

Miller, S.; 2000; *Geochemistry of ferruginous clogging of Karoo wells*; Unpublished MSc thesis; University of Cape Town, Cape Town

Parsons, R.; 2002; Recharge of Table Mountain Group aquifer systems; *A synthesis of the Hydrogeology of The Table Mountain Group- Formation of a research strategy*; Water Research Commission, South Africa; WRC report number TT 158/01

Rosewarne, P.; 2002; Hydrogeological characteristics of the Table Mountain Group aquifers; *A synthesis of the Hydrogeology of The Table Mountain Group- Formation of a research strategy*; Water Research Commission, South Africa; WRC report number TT 158/01

Smart, M.; Tredoux, G.; 2002; Groundwater quality and fitness for use; *A synthesis of the Hydrogeology of The Table Mountain Group- Formation of a research strategy*; Water Research Commission, South Africa; WRC report number TT 158/01

Smith, M.; 2003; *Personal Communication*

Smith, M.; 2002; *Research Proposal to NRF* (National Research Foundation), South Africa

Smith, M.; Clarke, S.; Cavé, L; 2002; *Chemical Evolution of Table Mountain Group groundwater and the source of iron*; Groundwater Division, Western Cape Conference; Tales of a Hidden Treasure; Somerset West

Smith, S.; Tuovinen, O.; 1985; Environmental analysis of iron-precipitating bacteria in groundwater and wells; *Groundwater Monitoring Review*, **5**, 4, pp.45-52

Stookey, L.; 1970; Ferrozine: A new spectrophotometric reagent for iron; *Anal. Chem.* **42**, pp.779-781

Straub, K.; Benz, M.; Schink, B.; 2001; Iron metabolism in anoxic environments at near neutral pH; *FEMS Microbiology Ecology*, **34** pp181-186

Tyrrel, S.; Howsam, P.; 1990; *Monitoring and prevention of iron biofouling in groundwater abstraction systems*; in Howsam, P.; Groundwater Engineering Conference, Granfield Institution of Technology, Granfield

Viollier, E.; Inglett, P.; Hunter, K.; Roychoudhury, A.; Van Cappellen, P.; 2000; The ferrozine method revisited: Fe(II)/Fe(III) determination in natural waters; *Applied Geochemistry*, **15**, pp.785-790

Yeld, J.; 2002: *Man vs. nature in a drying landscape*; Cape Argus; Thursday, July 25

APPENDIX

Table I: Borehole field data

					Absorbance		Concentration (µm/L)	
Borehole	**DO (%)**	**pH**	**EC (ms/cm)**	**Temp (°C)**	**Fe2+**	**Fe (tot)**	**Fe2+**	**Fe (tot)**
VR11	5	6.2	2.71	16.7	0.007	0.007	16	16
VR6	0	5.8	0.89	16.1	0.011	0.007	18	16
VG3	59	5.3	2.1	16.5	0.09	0.016	40	19
DP15	61	3.6	2.55	22.2	0.277	0.364	95	120
DP29	15	6.7	1.844	20.8	0.133	0.156	53	60
DP29filt	No data				0.122	0.138	50	54
KG1	32	6.1	4.39	21.5	No data			
DL16	35	6.2	4.8	19				
DL13	70	7.5	9.5	16.6				
DL17	45	7.2	5.66	20.3				

Table II: Ferrozine standard curve

	Conc (m/l)	Absorbance	Concentration (µm/L)
10	0.0001800	0.629	180
20	0.0000900	0.423	90
50	0.0000360	0.197	36
100	0.0000180	0.101	18
200	0.0000090	0.053	9

Table III: Borehole water analysed by ICP-MS (concentrations in ppb). (NIST is an external certified standard used to ascertain accuracy of results.)

	NIST -1640	certified	VG3	VR6	AHVR	KG1	DP15	DP29	DL13	DL16	DL17	PS
Li	48.9	50.7	8.45	0.70	1.58	45.7	15.5	18.9	73.0	49.1	50.3	0.95
Be	32.4	34.94	3.47	1.56	1.79	1.54	5.01	2.52	0.19	0.84	0.68	2.32
B	302	301.1	515	*n.d.*	*n.d.*	41.1	*n.d.*	*n.d.*	115	37.5	65.0	*n.d.*
Na	33124	29350	33556	14341	14595	44728	22614	25341	173046	63446	62244	2988
Mg	6085	5819	4075	1432	1616	10844	3652	3760	40101	11681	17215	581
Al	53.3	52.0	55.5	2.47	27.3	11.1	2226	3.36	143	8.44	20.4	111
Si	4471	4730	125	1837	2201	979	2194	1808	3082	3396	3302	*n.d.*
K	872	994	944	342	578	10128	2696	3403	26417	14816	17080	158
Ca	6783	7045	1924	1204	928	11694	2902	4269	37293	10608	17789	152
Ti	5.38	-	*n.d.*	*n.d.*	*n.d.*	8.85	2.52	2.75	27.5	8.88	15.9	*n.d.*
V	11.7	12.99	6.85	*n.d.*	*n.d.*	*n.d.*	*n.d.*	*n.d.*	44.6	*n.d.*	2.09	*n.d.*
Cr	29.0	38.6	10.2	5.57	1.07	0.82	2.99	11.5	2.86	6.44	1.39	5.54
Mn	111	121.5	208	3.53	32.1	1691	602	634	658	484	1753	4.28
Fe	17.0	34.3	6.16	82.3	32.2	5367	5293	1258	927	750	4078	20.8
Co	19.1	20.28	3.42	0.16	1.17	6.62	77.9	2.59	2.04	3.39	20.3	0.18
Ni	27.8	27.4	17.8	0.77	2.43	19.6	168	16.3	8.56	5.80	22.6	0.090
Cu	84.8	85.2	4.31	7.52	2.23	9.26	20.8	2.55	3.10	13.8	11.7	*n.d.*
Zn	61.6	53.2	58.4	27.1	16.9	302	1715	71.0	85.9	132	124	0.095
As	25.6	26.67	0.012	*n.d.*	0.24	0.29	7.49	0.26	1.96	1.26	0.48	*n.d.*
Se	21.7	21.96	0.28	*n.d.*	*n.d.*	0.71	1.51	0.98	2.70	1.38	0.70	*n.d.*
Rb	2.08	2.00	2.15	0.92	1.74	26.8	9.24	10.8	54.8	31.3	41.8	0.29
Sr	119	124.2	22.1	9.82	3.51	44.8	18.2	17.2	249	75.2	139	5.07
Zr	0.78	-	1.39	0.17	*n.d.*	0.023	0.080	0.13	0.32	0.059	0.25	0.13
Mo	47.7	46.75	0.047	0.070	0.042	0.036	0.086	0.064	0.72	0.38	0.78	0.018
Ag	7.22	7.62	0.94	0.21	0.36	0.76	0.31	0.22	0.41	0.24	0.35	0.52
Cd	22.1	22.79	0.067	0.016	0.049	0.23	2.55	0.040	0.77	0.22	0.55	*n.d.*
Ba	142	148.0	16.6	3.41	0.12	111	20.6	27.9	113	151	79.2	4.15
Hg	1.56	-	0.14	0.25	0.14	0.063	0.20	0.18	0.47	0.24	0.70	0.062
Pb	27.6	27.89	1.32	0.12	0.19	0.57	39.6	0.11	0.051	0.33	0.17	*n.d.*
Th	0.047	-	0.014	*n.d.*	*n.d.*	*n.d.*	0.87	*n.d.*	0.027	*n.d.*	0.030	0.039
U	0.64	-	1.22	0.070	0.38	0.11	39.9	0.11	0.29	0.13	0.033	0.024

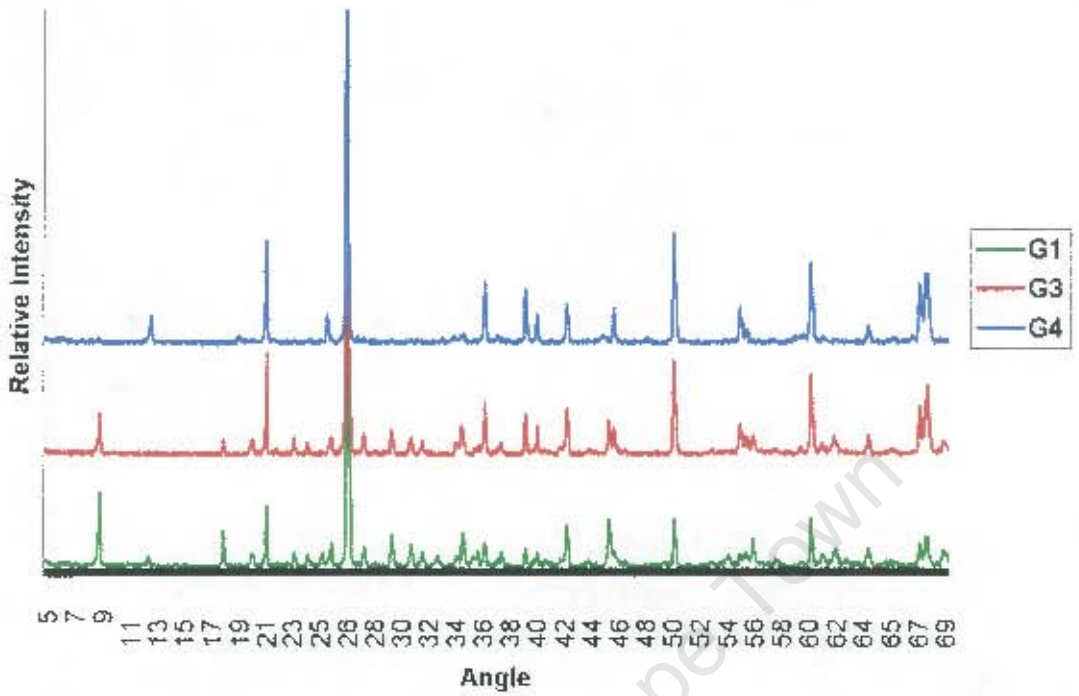

Figure I: XRD scans of Goudini samples

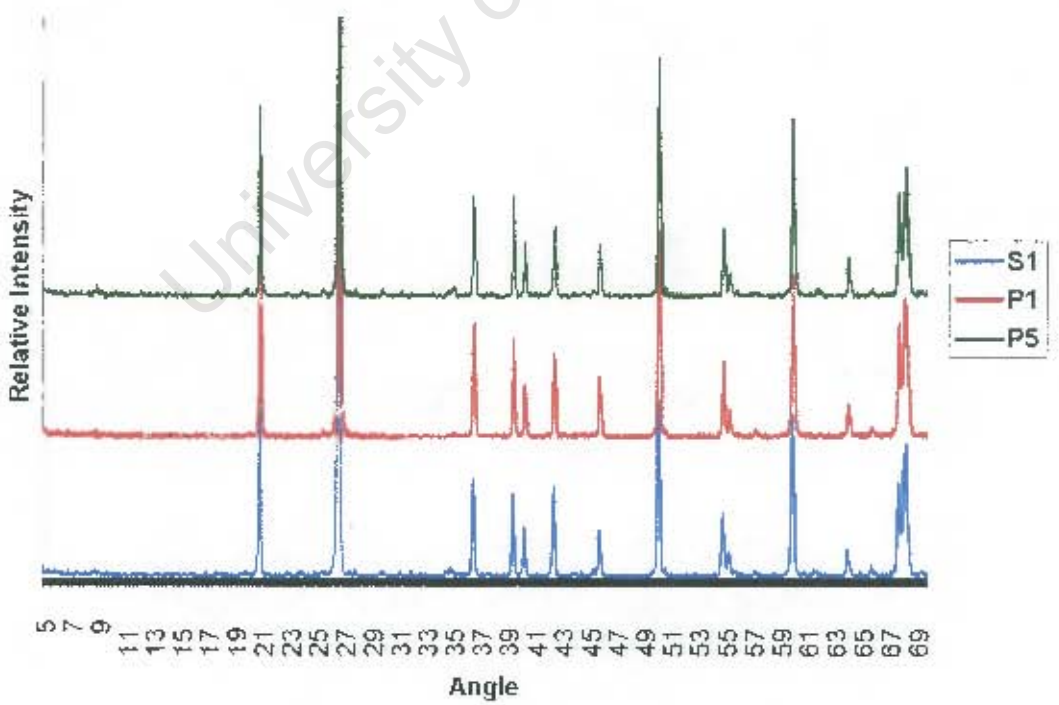

Figure II: XRD scans of Peninsula and Skurweberg samples

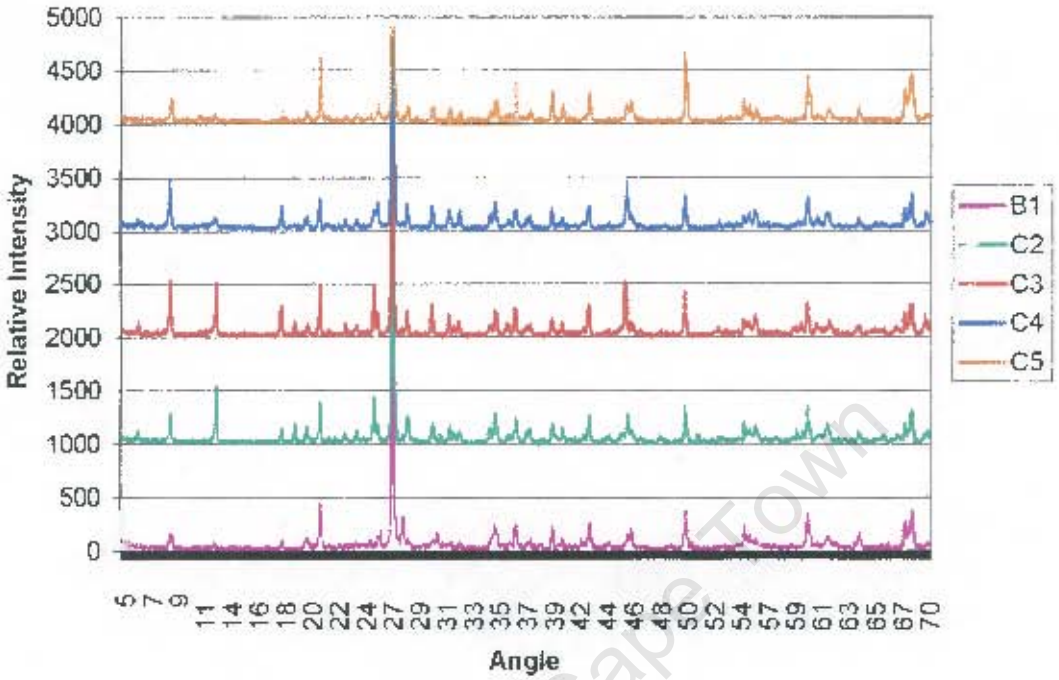

Figure III: XRD scans of Cedarberg and Bokkeveld samples

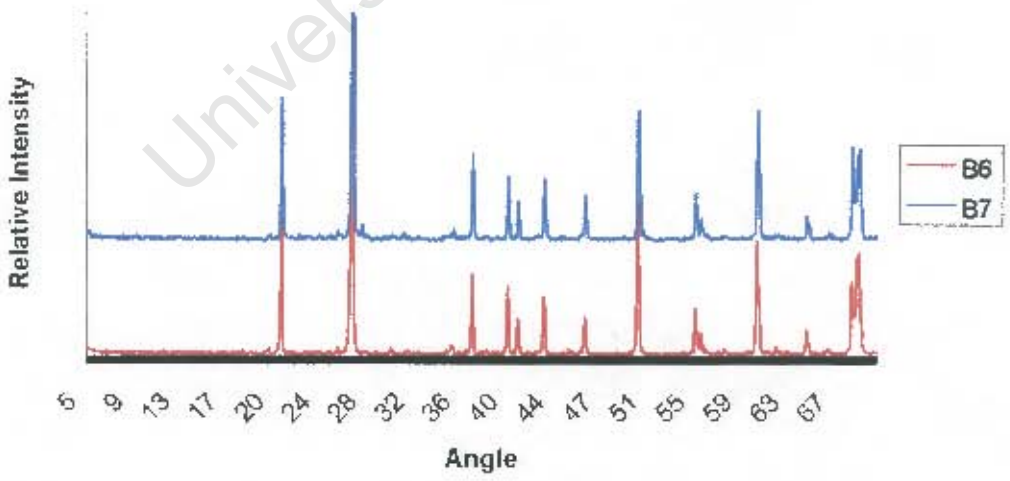

Figure IV: XRD scans of Baviaanskloof samples

Table IV: XRF data for rock samples (all values as mass percentage)

Sample	P1	P2	P3	P4	P5	P6	C1	C2	C3	C4	C5
SiO_2	97.385	95.575	96.743	96.225	93.256	98.059	61.913	59.636	57.266	57.629	72.258
$Al2O_3$	1.273	2.267	1.696	1.968	2.914	0.880	15.659	19.026	21.963	19.468	13.170
TiO_2	0.043	0.108	0.061	0.103	0.163	0.284	0.856	0.965	0.898	1.019	0.720
Fe_2O_3	0.391	0.529	0.495	0.469	0.896	0.594	6.821	6.445	6.502	6.814	5.438
MnO	0.017	0.021	0.022	0.021	0.026	0.017	0.067	0.043	0.138	0.045	0.055
MgO	0.166	0.275	0.220	0.220	0.270	0.190	1.836	2.605	1.674	2.221	1.221
CaO	0.014	0.025	0.017	0.019	0.023	0.021	1.401	0.029	0.021	0.250	0.054
Na_2O	0.171	0.124	0.132	0.098	0.214	0.171	0.300	0.791	0.284	0.306	0.231
K_2O	0.234	0.605	0.447	0.488	0.731	0.177	3.956	4.941	5.338	5.859	3.233
P_2O_5	0.008	0.014	0.012	0.012	0.031	0.016	1.230	0.121	0.121	0.420	0.054
SO_3	0.003	0.004	0.017	0.002	0.025	0.003	0.003	0.003	0.004	0.005	0.024
Cr_2O_3	0.015	0.008	0.008	0.008	0.015	0.010	0.019	0.017	0.026	0.022	0.016
NiO	0.004	0.004	0.004	0.003	0.007	0.004	0.006	0.005	0.009	0.008	0.003
H_2O^-	0.066	0.026	0.036	0.037	0.053	0.062	0.836	0.438	0.932	0.370	0.242
LOI	0.224	0.371	0.250	0.281	0.529	0.184	4.448	4.255	4.451	4.714	3.264
Total	100.013	99.956	100.159	99.954	99.152	100.670	99.351	99.320	99.627	99.149	99.983
S ppm	4.1	4.5	3.5	9.9	21.6	2.8	49.8	21.6	23.3	165.5	43.3

Sample	G1	G2	G3	G4	S1	S2	S3	B4	B6	B7	B1	B2
SiO_2	60.812	97.164	78.925	83.146	93.325	97.264	98.332	88.781	92.696	91.333	71.368	67.583
$Al2O_3$	20.196	1.057	11.990	5.219	3.115	1.667	0.787	6.176	3.408	5.031	13.823	16.676
TiO_2	0.918	0.333	0.587	0.569	0.196	0.109	0.164	0.096	0.262	0.161	1.159	0.964
Fe_2O_3	6.544	0.667	1.623	6.472	0.599	0.429	0.447	0.596	0.733	0.604	3.380	2.748
MnO	0.037	0.021	0.021	0.046	0.022	0.017	0.018	0.026	0.023	0.021	0.023	0.026
MgO	0.830	0.209	0.646	0.543	0.223	0.156	0.160	0.332	0.359	0.351	0.856	1.804
CaO	0.023	0.027	0.040	0.025	0.017	0.030	0.017	0.023	0.020	0.095	0.140	0.233
Na_2O	0.430	0.275	0.264	0.377	0.181	0.192	0.143	0.222	0.158	0.186	0.412	0.982
K_2O	5.844	0.204	3.846	0.622	0.787	0.082	0.029	1.955	0.786	1.697	5.648	4.074
P_2O_5	0.040	0.016	0.054	0.038	0.014	0.016	0.010	0.014	0.012	0.014	0.084	0.077
SO_3	0.012	0.005	0.003	0.023	0.003	0.004	0.003	0.002	0.002	0.004	0.011	0.004
Cr_2O_3	0.023	0.011	0.017	0.015	0.009	0.015	0.010	0.007	0.011	0.015	0.022	0.025
NiO	0.010	0.002	0.008	0.006	0.003	0.029	0.005	0.003	0.003	0.068	0.003	0.004
H_2O^-	0.114	0.074	0.032	0.124	0.076	0.040	0.023	0.059	0.240	0.067	0.661	0.725
LOI	3.224	0.200	2.024	1.777	0.564	0.291	0.160	0.996	0.996	0.709	2.680	3.751
Total	99.056	100.266	100.079	99.001	99.132	100.340	100.307	99.287	99.709	100.355	100.268	99.675
S ppm	101.5	1.6	22.5	193.1	3.4	136.9	53.5	59.5	13.6	29.1	426.4	90.2

Table V: Trial leaching experiment 1

Time (hrs)		C2 (ppm)	G1 (ppm)	C2 (µm/g)	G1 (µm/g)	C2 pH	G1 pH
	Blank	0.006	0.006	0.01	0.01	4.3	4.3
0	1	0.005	0.098	0.26	1.45	5.7	5.4
0.17	2	0.02	1.19	0.21	2.76	6.0	6.0
0.5	3	-0.003	0.345	0.32	0.89	6.0	5.8
1.17	4	-0.002	1.9	0.15	1.35	5.9	6.5
2.17	5	-0.003	0.006	0.23	1.21	6.0	5.0
4.17	6	No data	0.003	0.17	0.49	6.3	6.7
24.17	7	0.389	5.05	0.14	1.81	6.1	6.3
48.17	8	0.395	6.81	0.14	2.44	7.0	7.0
96.17	9	0.431	4.89	0.15	1.75	4.2	6.2
96.17	10	0.837	4.93	0.30	1.77	6.6	7.0

Table VI: Trial leaching experiment 2

Time (hrs)		C2 (ppm)	G1 (ppm)	C2 (um/g)	G1 (um/g)
	Blank	0.006	0.006	Bdl	Bdl
0	1	0.005	0.098	Bdl	0.04
0.17	2	0.02	1.19	Bdl	0.43
0.5	3	-0.003	0.345	Bdl	0.12
1.17	4	-0.002	1.9	Bdl	0.68
2.17	5	-0.003	0.006	Bdl	Bdl
4.17	6	No data	0.003	Bdl	Bdl

Table VII: Aerobic leaching experiment at pH 3 (all values in µm/l)

					Duplicates	
	C2	G1	B7	B1	C1	B7
0.166	0.07	0.12	0.66	0.06	0.06	
0.666	0.06	0.21	0.71	0.04		
1.666	0.16	0.13	0.66	0.03		
3.666	0.10	0.23	0.99	0.10		
5.666	0.17	0.55	1.14	0.01		
21.666	0.31	1.33	1.50	0.02		1.21
45.666	0.26	1.72	1.81	0.07		
93.666	0.41	1.60	1.26	0.02		
Total time	C1	G2	B4	B2		
	1.20	68.11	145.88	27.89		

Table VIII: Aerobic leaching experiment at pH 5 (all values in µm/l)

					Duplicates		
	C2	G1	B7	B1	G1	B1	Blank
0.166	0.01	0.07	0.04	0.03			0.02
0.666	0.01	0.11	0.04	0.03			
1.666	0.01	0.11	0.09	0.01			
3.666	0.02	0.06	0.10	0.00	0.10		
5.666	0.01	0.18	0.15	No data			
21.666	0.03	No data	0.35	0.01			
45.666	0.01	0.16	0.25	0.03		0.04	
93.666	0.01	0.09	0.18	0.02			
Total time	C1	G2	B4	B2			
	0.04	0.29	0.17	0.12			

Table IX: Aerobic leaching experiment using water from borehole DL17 (all values in µm/l)

					Duplicates		
	C2	G1	B7	B1	G1	B1	Blank
0.166	0.01	0.01	0.00	0.00			0.00
0.666	0.00	0.01	0.00	0.00	0.01		
1.666	0.00	0.01	0.01	0.00			
3.666	0.00	0.01	0.01	0.00			
5.666	No data	0.02	0.01	0.00			
21.666	No data	0.01	0.01	0.00			
45.666	0.01	0.02	0.02	0.00			
93.666	0.00	0.01	0.01	0.00		0.01	
Total time	C1	G2	B4	B2			
	0.01	0.02	0.02	0.01			

Table X: Aerobic leaching experiment using de-ionised water (all values in µm/l)

					Duplicates		
	C2	**G1**	**B7**	**B1**	**C1**	**B7**	**Blank**
0.166	0.01	0.04	0.01	0.05			0.00
0.666	Bdl	bdl	bdl	bdl			
1.666	Bdl	0.01	0.01	0.01		0.02	
3.666	Bdl	bdl	bdl	bdl			
5.666	Bdl	bdl	bdl	Bdl			
21.666	Bdl	0.06	0.02	0.05	0.01		
45.666	Bdl	0.00	0.00	0.00			
93.666	Bdl	0.48	0.02	0.12			
Total time	**C1**	**G2**	**B4**	**B2**			
	0.71	0.18	0.08	0.04			

Table XI: Anaerobic leaching experiment (all values in µm/l). Duplicates in brackets.

	P5	**C2**	**C1**	**G1**	**B7**	**B4**	**B1**	**B2**
MQ	0.18	0.116 (0.058)	0.156	2.85	11.6	3.79	0.082	0.923
DL17	0.087 (0.055)	0.065	0.078	6.54	14.9	3.16	0.064	3.9
pH 5		0.128	3.57	11.7	32.5 (11.7)	41.8	0.545	5.21
pH 3	6.57	5.97	0.17	27.2	41.6	No data	1.99	(14.4)

	P5	**C2**	**C1**	**G1**	**B7**	**B4**	**B1**	**B2**
MQ	0.02	0.01 (0.01)	0.01	0.25	1.04	0.34	0.01	0.08
DL17	0.01 (0.00)	0.01	0.01	0.58	1.33	0.28	0.01	0.35
pH 5	0.00	0.01	0.32	1.05	2.91 (1.05)	3.74	0.05	0.47
pH 3	0.59	0.53	0.02	2.43	3.72	No data	0.18	0.00 (1.29)

Table XII: Statistical analysis of ICP-MS data.

Element	Measured value	NIST-1640 certified value	Standard Deviation	Coefficient of variation
Li	48.9	50.7	1.275648	2.561
Be	32.4	34.94	1.781126	5.288
B	302	301.1	0.925301	0.306
Na	33124	29350	2668.863	8.543
Mg	6085	5819	188.2723	3.163
Al	53.3	52.0	0.885548	1.682
Si	4471	4730	183.0999	3.979
K	872	994	86.48019	9.270
Ca	6783	7045	185.423	2.681
Ti	5.38	-	-	-
V	11.7	12.99	0.891602	7.213
Cr	29.0	38.6	6.79364	20.101
Mn	111	121.5	7.280144	6.256
Fe	17.0	34.3	12.22379	47.644
Co	19.1	20.28	0.812384	4.122
Ni	27.8	27.4	0.291512	1.055
Cu	84.8	85.2	0.288212	0.339
Zn	61.6	53.2	5.939667	10.347
As	25.6	26.67	0.724202	2.768
Se	21.7	21.96	0.159833	0.731
Rb	2.08	2.00	0.059314	2.904
Sr	119	124.2	3.511526	2.884
Zr	0.78	-	-	-
Mo	47.7	46.75	0.641747	1.359
Ag	7.22	7.62	0.279372	3.763
Cd	22.1	22.79	0.485288	2.161
Ba	142	148.0	4.380617	3.023
Hg	1.56	-	-	-
Pb	27.6	27.89	0.219939	0.793
Th	0.047	-	-	-
U	0.64	-	-	-

Table XIII: Statistical analysis of leaching experiment data.

Value1	Value 2	Standard deviation	Coefficient of variation
Leaching aerobic			
0.07	0.06	0.003792	5.917
1.50	1.21	0.208575	15.402
0.06	0.10	0.032234	39.412
0.03	0.04	0.001707	4.7551
0.01	0.01	0.002212	29.639
0.00	0.01	0.002402	40.104
0.01	0.02	0.007205	67.739
0.02	0.01	0.006131	46.818
Leaching anaerobic			
0.01	0.00	0.002023	31.869
0.01	0.01	0.003666	47.140
2.91	1.05	1.314654	66.551
0.00	1.29	0.910145	141.421
			44.730